



Diplomarbeit

Feedback-based LTE-Downlink Measurements

ausgeführt zum Zwecke der Erlangung des
akademischen Grades eines Diplom-Ingenieurs

unter der Leitung von
Univ. Prof. Dipl.-Ing. Dr.techn. Markus Rupp
Dipl.-Ing. Martin Lerch
Institute of Telecommunications

eingereicht an der Technischen Universität Wien
Fakultät für Elektrotechnik und Informationstechnik

Martin Klaus Müller, B.Eng.

Matr. Nr.: 1026943

Hauslabgasse 14/23, 1050 Wien, Österreich

Wien, im November 2013

I hereby certify that the work reported in this thesis is my own,
and the work done by other authors is appropriately cited.

Martin Klaus Müller
11.11.2013

Abstract

The predictions for cellular traffic in the next few years show an exponential growth for mobile data. New transmission techniques and the application of efficient algorithms are required in order to make the best use of the scarce resources in mobile communications to be able to satisfy this growing demand.

Following the evolution of mobile cellular systems, the last releases of UMTS¹ were already capable of applying MIMO²-techniques to significantly increase the possible throughput per cell. This trend went on with the introduction of LTE³ and its successor LTE-A⁴. Even more antennas are supported and the system gets more flexible by providing a large set of predefined modulation and coding schemes. Thus each link can be used with close to optimal transmission-parameters.

The Vienna MIMO Testbed was designed to measure the performance of various wireless transmission standards. Up to now, this was achieved without using a feedback link. However, very flexible LTE and LTE-A transmission-modes cannot be evaluated this way. To overcome these restrictions, a feedback mechanism has been integrated in the testbed. This allows to measure advanced features and transmission modes of LTE and LTE-A.

How this feedback is incorporated for the measurement of such advanced modes is described in this thesis. Topics under investigation are the impact of retransmissions on throughput and block error ratio, frequency selective scheduling and the performance of advanced transmission modes, such as CLSM⁵ and MU-MIMO⁶ techniques. The adaptation of the testbed-software for measuring the aforementioned aspects is detailed in this work. For every transmission mode, measurement results are provided.

¹Universal Mobile Telecommunications System

²Multiple Input Multiple Output

³Long Term Evolution

⁴LTE-Advanced

⁵Closed Loop Spatial Multiplexing

⁶Multi User MIMO

Kurzfassung

Für das Daten-Aufkommen in zellulären Mobilfunknetzen wird ein exponentielles Wachstum vorhergesagt. Neue Übertragungstechniken und der Einsatz von effizienten Algorithmen sind notwendig, um den größten Nutzen aus den spärlich vorhandenen Ressourcen zu ziehen, um so den wachsenden Bedarf zu befriedigen. Vielversprechend ist der Einsatz von MIMO¹-Techniken. Sie ermöglichen es, den Datendurchsatz in einer Zelle deutlich zu erhöhen. In dem Mobilfunkstandard LTE² und dessen Nachfolger LTE-A³ wurde der Einsatz von MIMO ausgeweitet. Noch mehr Antennen können eingesetzt werden und das System wird flexibler durch die Bereitstellung einer großen Anzahl von vordefinierten Modulations- und Codierungs-Arten. So kann jeder Übertragungspfad annähernd optimal genutzt werden.

Das Vienna MIMO Testbed wurde entworfen, um die Leistung von unterschiedlichen Mobilfunk-Standards messtechnisch zu ermitteln. Bis jetzt war dazu keine Rückführung von Informationen vorgesehen. Sehr flexible Übertragungs-Modi von LTE und LTE-A können so aber nicht untersucht werden. Um diese Einschränkungen aufzuheben, wurde eine solche Rückführung von Informationen in den Messaufbau integriert. Dadurch wird die Messung von fortschrittlichen Mechanismen und Übertragungs-Modi von LTE und LTE-A ermöglicht.

Wie diese zurückgeführten Informationen in Verbindung mit solchen fortschrittlichen Modi in die Messung eingebunden werden, wird in dieser Arbeit beschrieben. Untersuchte Themen sind der Einfluss von Sendewiederholungen auf den Datendurchsatz, Frequenz-selektive Ressourcen-Verteilung und die Leistungsfähigkeit von fortschrittlichen Übertragungs-Modi wie CLSM⁴ und MU-MIMO⁵-Techniken. Wie die Software des Messaufbaus für die Messung der soeben genannten Aspekte angepasst werden muss, wird in dieser Arbeit erläutert. Für jeden Übertragungs-Modus werden Messergebnisse in der Arbeit vorgestellt.

¹Multiple Input Multiple Output

²Long Term Evolution

³LTE-Advanced

⁴Closed Loop Spatial Multiplexing

⁵Multi User MIMO

Acknowledgements

My first words of gratitude extend to my supervisor, Prof. Markus Rupp. It was he who made this work possible and was always there to provide support and advice when necessary.

I would like to thank my second supervisor, Martin Lerch, who helped me understand my work in depth by discussing even the smallest detail.

My thanks also go to my colleagues at the Institute of Telecommunications, especially Stefan Schwarz for the invaluable support with simulation-issues.

My special thanks go to my good friend and colleague Michael Meidlinger, on whose work this thesis is based upon. Thank you for never being short of an answer, no matter what the problem is!

Finally, and most importantly, I want to thank my friends and my family, especially my parents, for being a continuous source of support and for being there, when I need them most.

Contents

1	Introduction	1
2	Theoretical Background	3
2.1	LTE Physical Layer	3
2.1.1	OFDM	3
2.1.2	MIMO	6
2.1.3	Channel Coding and HARQ	8
2.1.4	Adaptive Modulation and Coding	11
2.2	LTE MAC-Layer	12
2.2.1	Feedback	12
2.2.2	Scheduling	13
2.2.3	LTE Transmission-Modes	15
3	Measurement Setup and Methodology	19
3.1	Vienna MIMO Testbed	19
3.1.1	Hardware	20
3.1.2	Software	21
3.2	Simulation Environment	21
3.2.1	LTE-Simulator	21
3.2.2	Simulator - Testbed Interface	23
3.2.3	Measurement Emulation	24
3.3	Measurement Methodology	24
3.3.1	Measurement/Simulation Process	26
3.3.2	Data Generation	28
3.3.3	Offline Evaluation	29
3.4	Implementation of LTE-Modes	30
3.4.1	Implementation Differences	30
3.4.2	Scheduler Implementation	31

4	Measurement- and Simulation-Results	37
4.1	Comparison of Different Scheduling Granularities	37
4.1.1	LTE Transmission-Mode 4, CLSM	37
4.1.2	LTE-A Transmission-Mode 9, CLSM	38
4.2	HARQ-Performance	39
4.3	ZF MU-MIMO	41
5	Conclusion and Outlook	43
	Bibliography	45
A	Acronyms	48

Chapter 1

Introduction

Since the first commercial deployment of Long Term Evolution (LTE), the successor of Universal Mobile Telecommunications System (UMTS), already several years have passed. But the evolution of mobile communication has not stopped then and first LTE Advanced (LTE-A) systems are about to be rolled out. This new standard is equipped with several new features, further enhancing the performance in order to keep pace with the always growing demand for more data rate. Since there is almost no practical experience with LTE-A, the search for new algorithms suited for the new environment and capable of exploiting the new structure is quite prevalent in research and is mostly pursued by employing numerical simulations for evaluation-purposes.

Simulation results are a good way to check the feasibility of new algorithms, but measurements under realistic circumstances are necessary to evaluate the performance in a real mobile communication system. Only there, the effect of all aspects that have not been modelled or have been abstracted for the simulations can be identified. The Vienna MIMO Testbed as described in [6], [12] can be used for the measurements of various mobile communication standards, among them the LTE-downlink. An example for such measurements can be found in [16]. There, the first part of the measurement-procedure is to transmit signals for all possible sets of transmission parameters for every measurement point. The optimal set is determined afterwards, by evaluating all received files and choosing those that yield the highest throughput for every transmission-constellation. While the advantage of this approach is, that no real-time feedback is necessary, there are two factors that restrict the measurement to certain transmission modes. For a transmission mode with a discrete set of transmission-parameters, the number of combinations that have to be transmitted is limited, but the computational effort can get out of hand. For the current hardware used for the offline evaluation, not

even all LTE transmission modes can be measured with the evaluation not taking an excessive amount of computation time. While theoretically still possible, LTE-A introduces new transmission modes, where the transmission parameters are no longer taken from a discrete set, but can take on continuous values. To measure these transmission modes, real-time feedback is necessary. The work done in [19] aims at providing real-time feedback in the Vienna Multiple Input Multiple Output (MIMO) Testbed in form of a software extension. With that knowledge, more transmission modes and features of LTE and LTE-A can be measured, what has not been performed before because of one of the two aforementioned reasons. In this work, the enhanced capabilities of the testbed are used to evaluate modes and features that are available now because of the reduced computational effort, e.g., the performance of Hybrid ARQ (HARQ) and closed loop transmissions. The other group of transmission modes under investigation implicitly needs feedback to generate the transmit-signal, e.g., frequency selective scheduling and advanced LTE-A transmission-modes like Multi User MIMO (MU-MIMO), which allows an evolved Node B (eNodeB) to schedule several User Equipments (UEs) on the same time-frequency resource. The focus of this work is the optimal filling of the available resources, involving the feedback and scheduling, what differences exist between the different modes and how these differences are reflected in the implementation in connection with the testbed.

The document is structured as follows: The theoretical background of LTE is explained in Chapter 2. On the physical layer, mostly the structure of the available resources and how the data is processed to be filled in the resource grid is of interest. What information is available on higher layers to fill the resources in an optimal fashion, i.e., the feedback, is explained afterwards as well as how the scheduler processes that information. The different LTE-modes are explained with an emphasis on the modes that are further investigated in later parts of this work. Chapter 3 contains a description of the testbed hardware and the software used for simulation and emulation of the LTE-environment. The implementation of the different LTE-modes is also explained here, with the major difference between them being the implementation of the feedback and the scheduler. Simulation results as well as the results from the measurements are presented in Chapter 4. The performance of the different modes in several configurations are compared regarding throughput and error-performance. Finally, the conclusions of this work are drawn in Chapter 5.

Chapter 2

Theoretical Background

To define the technical environment in which this work is settled, the basics of LTE-communication are detailed in this chapter. The first section will deal with the basics of the physical layer of LTE-transmission. It is explained what resources are available and how they are structured and categorized. How the data bits chosen for transmission are processed is also stated. The concepts explained first are needed in the second section, where it is then discussed, how the distribution of resources among the users is executed, what information is necessary to perform elaborate choices and what different strategies exist and how they are connected with the LTE-standard.

2.1 LTE Physical Layer

One big shift in paradigm from UMTS to LTE is the change in the physical layer from Code Division Multiple Access (CDMA) to Orthogonal Frequency Division Multiple Access (OFDMA). As a consequence, the resources are no longer organized in a code-time domain, but in a frequency-time grid. Because the organization, structure and distribution of resources is a vital topic in this work, the new resource-structure in LTE and other resource-related aspects on the physical layer are discussed in the following.

2.1.1 OFDM

The transmission scheme used in the LTE-downlink is Orthogonal Frequency-Division Multiplexing (OFDM), which is also the case for a variety of other standards for wireless transmission, such as WiMAX or DVB broadcast systems. The total bandwidth of OFDM is subdivided into many subcarriers, why it is also re-

ferred to as a multi-carrier transmission scheme. The OFDM transmit signal $x(t)$ for a certain time-interval m of length T_S (corresponding to the symbol duration) can be expressed in complex baseband notation as

$$s(t) = \sum_{k=0}^{N_c-1} s_k(t) = \sum_{k=0}^{N_c-1} a_k^{(m)} e^{j2\pi k \Delta f t}, \quad (2.1)$$

where N_c corresponds to the total number of subcarriers, $s_k(t)$ represents the signal transmitted on sub-carrier k with frequency $k\Delta f$ and $a_k^{(m)}$ corresponds to the modulation symbol transmitted on subcarrier k during the time-interval m . As Equation (2.1) shows, for each time interval of length T , all subcarriers transmit in parallel a total of N_c modulation symbols. Thus, the broadband frequency selective channel is divided into a set of orthogonal frequency flat channels for each subcarrier. The modulation of each subcarrier is independent of all the others, with modulation symbols from an arbitrary symbol alphabet (e.g., 16-QAM or 64-QAM). This structure allows for a high density of subcarriers without interfering each other. For more details on the PHY-layer capabilities of OFDM, refer to [9]. An important aspect of OFDM for this work is how it structures the transmission resources in a time-frequency grid. It is shown in Figure 2.1. Depicted there is a

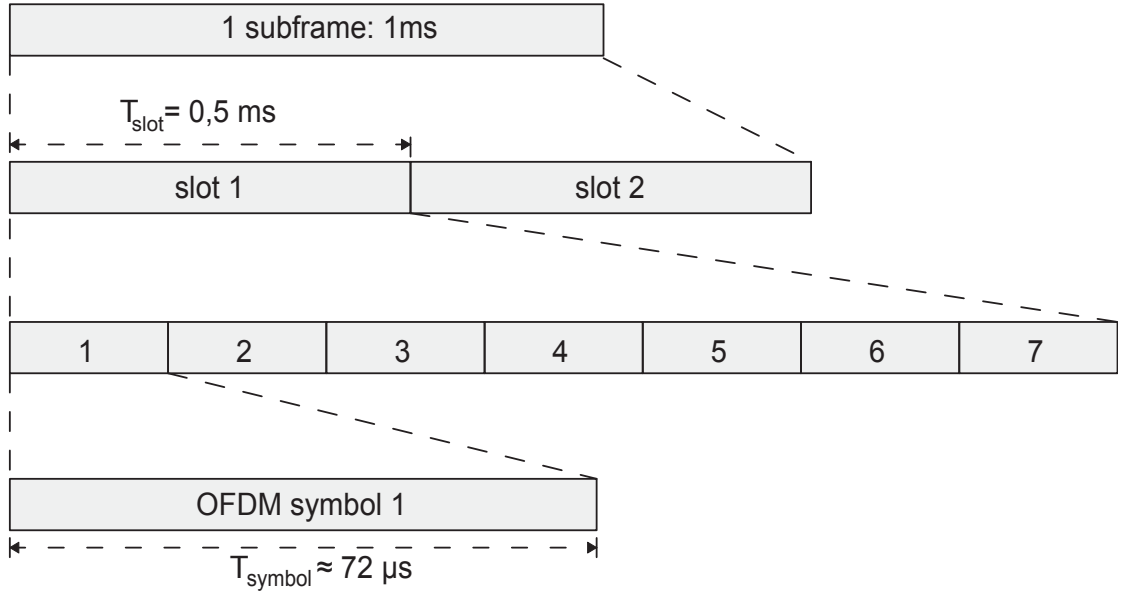


Figure 2.1: Time structure of one LTE subframe.

so-called *subframe* with 1 ms duration. The subframe is subdivided in two slots with 0.5 ms duration. The smallest unit in the time-domain is the duration of one OFDM-symbol, $T_S \approx 72 \mu\text{s}$. Therefore, each slot is divided in $N_S = 7$ OFDM-symbols. In the frequency-domain the whole system bandwidth is divided into

System bandwidth, B_{Ch} [MHz]	1.4	3	5	10	15	20
Number of RBs, N_{RB}	6	15	25	50	75	100
Number of subcarriers, N_c	72	180	300	600	900	1200
Transmission bandwidth, B_{TX} [MHz]	1.08	2.7	4.5	9	13.5	18
Relative guardband size	23%	10%	10%	10%	10%	10%

Table 2.1: Available resources for different LTE system bandwidths [1] .

N_c subcarriers, where the subcarrier spacing for LTE-systems is 15 kHz. The full resource-grid is shown in Figure 2.2. $N_{c,RB} = 12$ subcarriers combined over one

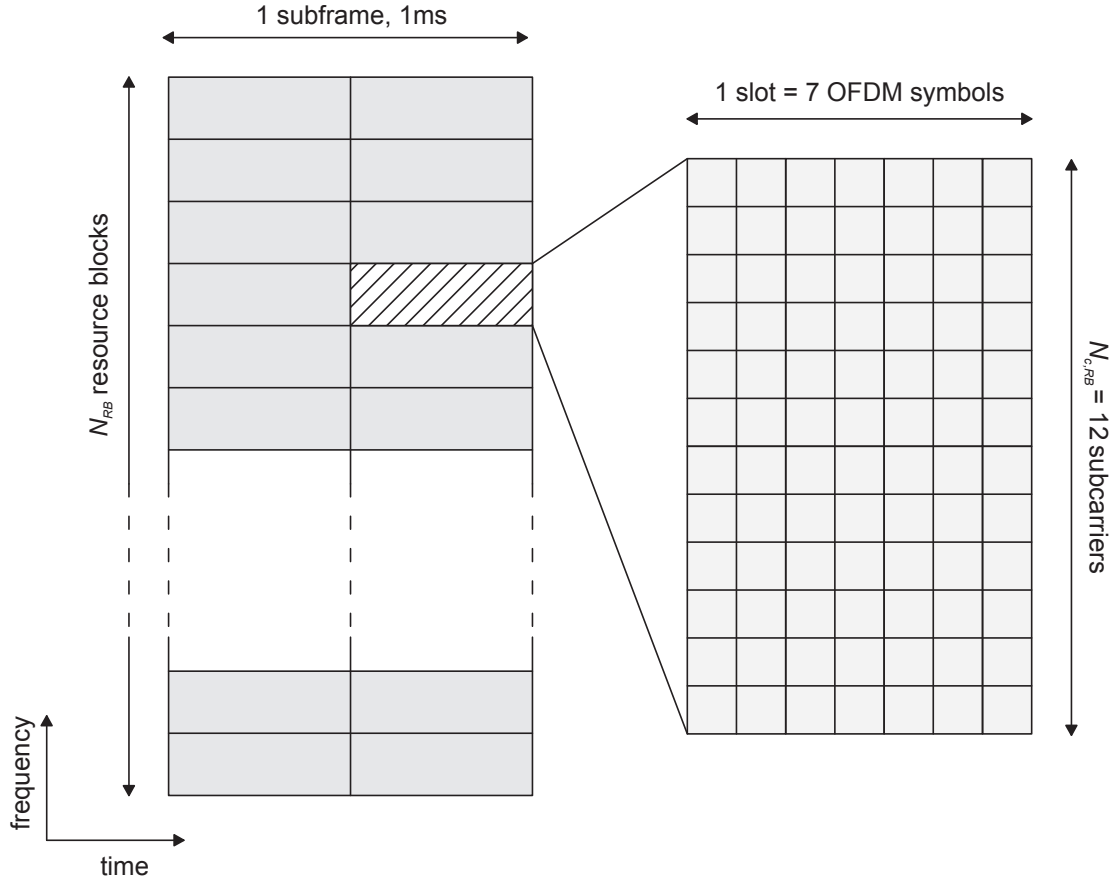


Figure 2.2: The LTE resource-grid over time and frequency [2].

slot form a Resource Block (RB). It results, that one RB contains $N_{c,RB} \cdot N_S = 12 \cdot 7 = 84$ OFDM-symbols. One RB is the finest granularity for, e.g., feedback or scheduling as it will be discussed later (Section 2.2). The possible system bandwidths B_{Ch} defined in the LTE-standard are shown in Table 2.1. There, also the total number of RBs N_{RB} for a given bandwidth and the resulting number of subcarriers $N_c = N_{RB} \cdot N_{c,RB}$, the actual transmission bandwidth B_{TX} and the relative guard-band size are listed.

2.1.2 MIMO

The performance of Single Input Single Output (SISO)-transmission can clearly be outperformed with the application of more than just one antenna on the transmitter- and receiver-side. Multiple transmit-antennas $N_{TX} > 1$ (Multiple Input Single Output (MISO)) yield transmit-diversity (by, e.g., applying an Alamouti scheme [4]), multiple receive-antennas $N_{RX} > 1$ (Single Input Multiple Output (SIMO)) allows for receive-diversity schemes, such as Maximum Ratio Combining (MRC). Having more than one antenna on both sides (MIMO) allows to achieve an even higher diversity gain. Applying diversity techniques is especially helpful in the low Signal to Noise Ratio (SNR)-region, to improve the link-quality. Another technique to improve the link-quality is beam-forming. This can be done by phase-aligning the signals on the transmit-antennas and thus increasing the received signal-power. However, the big achievement of MIMO is the multiplexing

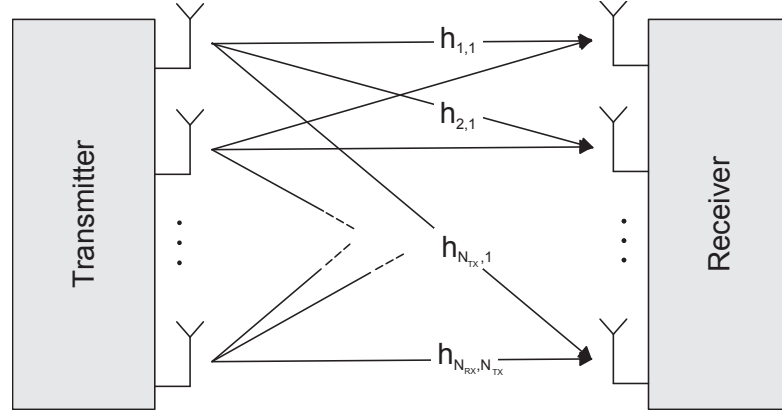


Figure 2.3: MIMO setup.

gain, that allows to transmit multiple streams (termed *layers* in LTE) on the same RB, thus enabling Spatial Multiplexing (SM) and improving the capacity linearly with the minimum number of antennas on each side. Because with a higher number of layers some interference is introduced between them, SM demands a higher SNR, so that the Block Error Ratio (BLER) does not get excessively high.

Reconsidering Figure 2.2, the application of MIMO leads to a certain depth of the resource elements, i.e., a maximum of $\min(N_{TX}, N_{RX})$ OFDM-symbols can be transmitted on the same frequency at the same time, as shown in Figure 2.4. This leads to several parallel time signals $s_k(t)$ (Equation (2.1)), resulting in the time signal vector $\mathbf{s}_k(t)$.

In an $N_{TX} \cdot N_{RX}$ MIMO-setup, as shown in Figure 2.3, for every pair of transmit- and receive-antennas, the transmission is characterized by an impulse response.

With the insertion of a cyclic prefix to every OFDM-symbol, thus cancelling the in-

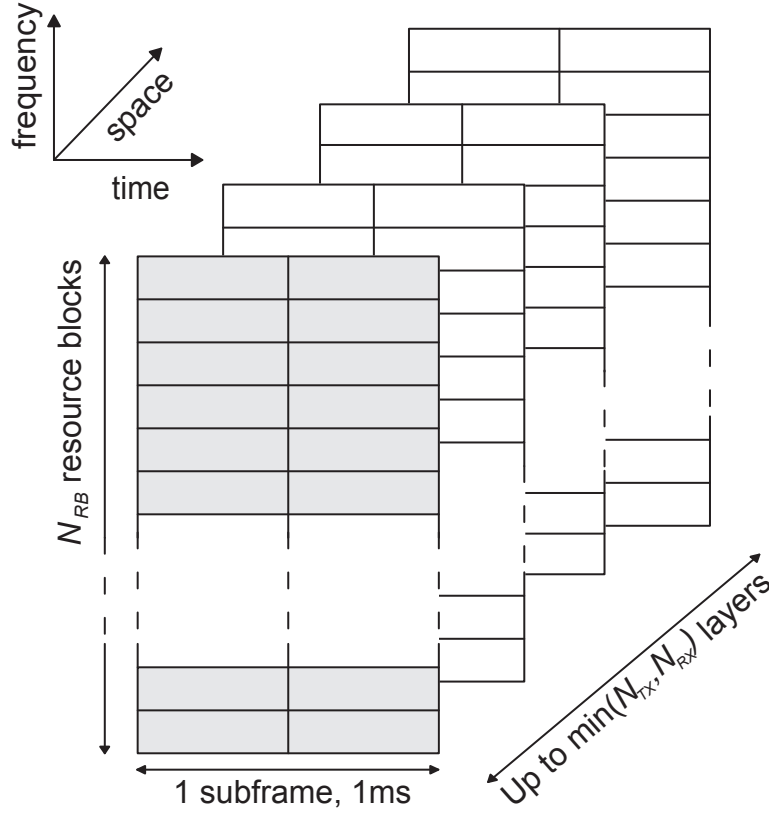


Figure 2.4: The LTE resource grid for a MIMO-setup, introducing the third spatial dimension.

ter symbol interference, the input-output relation per antenna-pair and subcarrier is characterized by only one coefficient. It is then possible to combine the coefficients for all antenna-pairs in one equation per subcarrier (considering discrete symbols):

$$\mathbf{y}_k = \mathbf{H}_k \mathbf{x}_k, \quad (2.2)$$

with

$$\mathbf{H}_k = \begin{pmatrix} h_{k,1,1} & h_{k,1,2} & \cdots & h_{k,1,N_{TX}} \\ h_{k,2,1} & h_{k,2,2} & \cdots & h_{k,2,N_{TX}} \\ \vdots & \vdots & \ddots & \vdots \\ h_{k,N_{RX},1} & h_{k,N_{RX},2} & \cdots & h_{k,N_{RX},N_{TX}} \end{pmatrix} \quad (2.3)$$

The number of spatial streams, e.g., the number of symbols that are transmitted in parallel, is not necessarily as large as the number of transmit antennas. To map the spatial layers to the transmit antennas is the task of the *Precoder*. It can be described by a so called Precoding Matrix \mathbf{W} and transforms the symbol vector \mathbf{s} into the transmit vector \mathbf{x} by

$$\mathbf{x}_k = \mathbf{W}_k \mathbf{s}_k, \quad (2.4)$$

where the number of elements in \mathbf{s} ($\hat{=}\lambda$) equal the number of spatially multiplexed streams and the number of elements in \mathbf{x} ($\hat{=}\tau$) equal the number of transmit antennas N_T , with the restriction $\lambda \leq \tau$ and the size of $\mathbf{W} \hat{=}\tau \times \lambda$. The combination of Equation (2.1) and Equation (2.2) leads to

$$\mathbf{y}_k = \mathbf{H}_k \mathbf{x}_k = \mathbf{H}_k \mathbf{W}_k \mathbf{s}_k, \quad (2.5)$$

with the product $\mathbf{H}_k \mathbf{W}_k$ also being called the *effective channel*, that the symbol vector \mathbf{s}_k experiences. There are several strategies of choosing the precoding matrix \mathbf{W} - the ones relevant for our work will be explained in Section 2.2.1 and Section 2.2.3.

2.1.3 Channel Coding and HARQ

As in almost all mobile communication systems, also LTE uses channel coding to protect the data from errors in noisy environments and correct them, i.e., a Forward Error Correction (FEC)-code is applied. Another task is to recognize erroneous bits and to report a erroneous transmission, i.e., Automatic Repeat reQuest (ARQ).

Channel Coding in LTE

The data bits chosen for joint transmission are first grouped in a Transport Block (TB). This TB is then appended with a Cyclic Redundancy Check (CRC)-code of 24 bits. If the total length exceeds 6144 bits, the TB is split up into several Code Blocks (CBs) for each of which another CRC-code is calculated and appended at the end of each block. In order for a TB to be considered as transmitted without error, the TB's as well as all of the CBs' CRC-codes have to be correct after decoding on the receiver side. If that is the case, the transmitter is notified by sending a positive ACKnowledgment (ACK). If the CRC is in error, all the received data in this TB is discarded and the receiver sends a Negative Acknowledgment (NAK)-message to the transmitter. After the CRC calculation and a potential segmentation, the TB (or each CBI individually in the case of segmentation), the data bits and the corresponding CRC-bits are coded together. LTE uses turbo coding [5] for channel coding. The turbo encoder consists of two rate $1/2$ coders what yields a combined coding rate of $1/3$. The rate matching to adjust the code rate of the original codeword to any desired rate is done by puncturing. This is important for HARQ (see next section) and for Adaptive Modulation and Coding (AMC), described in Section 2.1.4.

$\lambda \rightarrow \# \text{ codewords}$	codeword-to-layer mapping
$1 \rightarrow 1$	codeword 1 \rightarrow layer 1
$2 \rightarrow 1$	codeword 1 \rightarrow layers 1,2
$2 \rightarrow 2$	codeword 1 \rightarrow layer 1 codeword 2 \rightarrow layer 2
$3 \rightarrow 1$	codeword 1 \rightarrow layers 1,2,3
$3 \rightarrow 2$	codeword 1 \rightarrow layer 1 codeword 2 \rightarrow layers 2,3
$4 \rightarrow 1$	codeword 1 \rightarrow layers 1,2,3,4
$4 \rightarrow 2$	codeword 1 \rightarrow layers 1,2 codeword 2 \rightarrow layers 3,4
$5 \rightarrow 2$	codeword 1 \rightarrow layers 1,2 codeword 2 \rightarrow layers 3,4,5
$6 \rightarrow 2$	codeword 1 \rightarrow layers 1,2,3 codeword 2 \rightarrow layers 4,5,6
$7 \rightarrow 2$	codeword 1 \rightarrow layers 1,2,3 codeword 2 \rightarrow layers 4,5,6,7
$8 \rightarrow 2$	codeword 1 \rightarrow layers 1,2,3,4 codeword 2 \rightarrow layers 5,6,7,8

Table 2.2: Mapping from layers to codewords [2].

In the case of MIMO-transmission over more than one layer, the data-bits are divided in up to two parallel data streams. All data-bits belonging to one data stream are coded together in one *codeword* (corresponding to one TB). The codewords are then mapped to the λ layers, which are mapped to the N_T transmit antennas by the Precoding Matrix (PM). The mapping from codewords to layers is shown in Table 2.2. From the possible codeword-to-layer mapping shown in the table, we do not consider the cases where multiple layers for one user are mapped to only one codeword (line 2,4,6). For LTE, the same mapping is valid, without the last four lines, because only up to four layers are supported by its Reference Signal (RS)-structure.

Hybrid ARQ

Primary, an ARQ-protocol is used to detect and report erroneously transmitted data-packets. Such errors can occur even if the appropriate Modulation and Coding Scheme (MCS) was used, because of, e.g., receiver noise or random fading changes. The packets in error are detected with the help of the aforementioned CRC-codes. HARQ implies, that the transmitted data is coded with an FEC code. Thus, even though bit-errors occurred during the transmission, all original input-bits in the coder including the CRC might be detected correctly due to the error-correction capabilities of the channel code. Only if after the decoding the CRC is still not correct, the packet is reported as corrupted and a new transmission is requested.

As we have seen in Section 2.1.3, both criterias for HARQ are fulfilled in LTE, because CRC-codes are used for error-detection and turbo-codes have a high performance in FEC. In LTE a combination of the two basic HARQ-modes is utilized.

The most obvious option is simply retransmitting the same packet that has been sent originally. By doing so, only the SNR per bit is improved, not the coding gain. This retransmission scheme is known as *Chase combining* [8]. The second option is to generate a codeword that is much longer than the number of bits, that is transmitted in one channel-use. At first one part of this codeword, that can be decoded independently, is transmitted. If a retransmission is requested, additional redundancy bits are transmitted, thus lowering the effective code rate and improving the coding gain. This technique can be termed *full* Incremental Redundancy (IR), while IR also in general allows overlapping (re-)transmissions. To combine these two options, several redundancy versions are generated from the original rate $1/3$ code word by puncturing. The code rate of the first TB is the

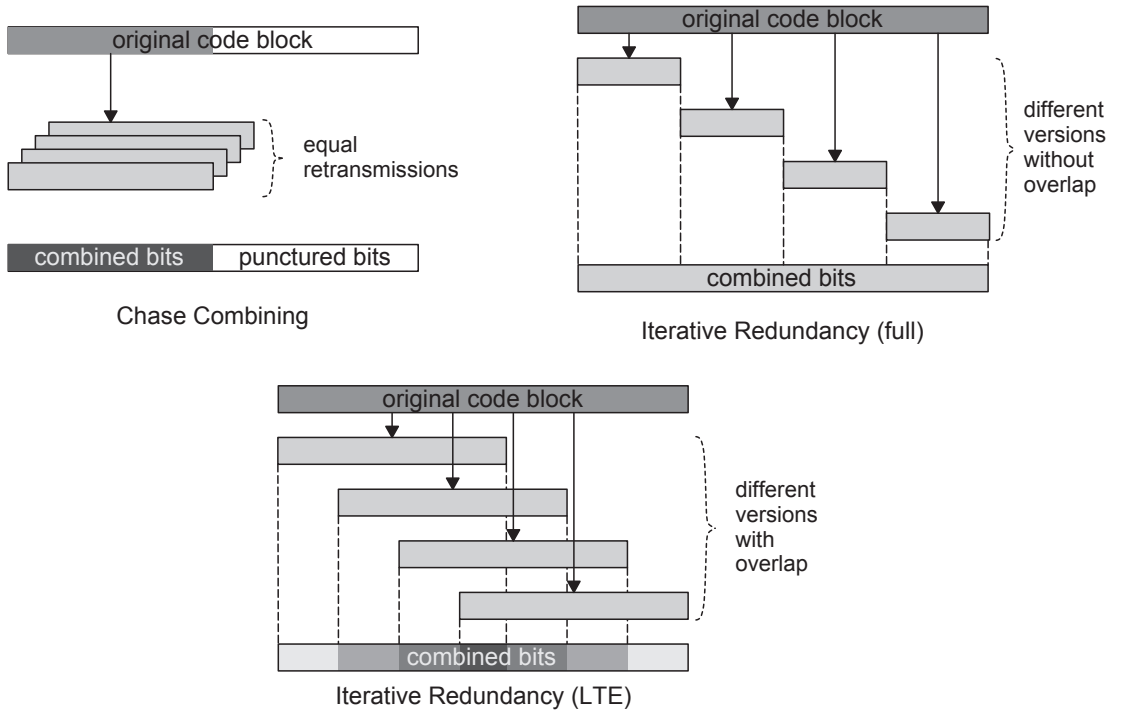


Figure 2.5: Different types of HARQ.

desired rate for the particular transmission. Each retransmission version contains already transmitted bits as well as new bits. On the receiver side, the decoding is always done jointly for all received packets (original transmission and all retransmission). Since the combined code rate is lowered with each retransmission, the whole transmission benefits from a higher coding gain. On the other hand, the combined calculation of the Log Likelihood Ratios (LLRs) for the bits that have been sent multiple times further decreases the Bit Error Ratio (BER). After the receiver has sent a NAK-report for $N_{RT,max}$ times (the maximum of allowed retransmission), there are no more attempts to transmit the data in question. The

different possibilities for HARQ are shown in Figure 2.5.

Not only does the utilization of HARQ provide an explicit adaptation of the coding rate, it also plays an important role in the combination with higher layer (end-to-end) protocols, such as TCP. If bit errors are not corrected, the higher layer protocol will recognize this and take its own measures to ensure that the whole data is received correctly, thus leading to, e.g., reduced data-rate, large retransmissions and increased overhead and delay. If the errors are already detected *and* corrected by the HARQ-protocol, the transmission appears to be error-free for higher layer protocols.

2.1.4 Adaptive Modulation and Coding

The changing characteristics of the transmission-channel in mobile communication networks make it necessary to dynamically adapt the modulation order as well as the coding rate. The main parameters that influence the total throughput are user data rate and the corresponding BLER. Both of these parameters are conversely affected by the modulation order and the coding rate, as it is shown in Figure 2.6.

A higher modulation order and coding rate (transmitting with the same average

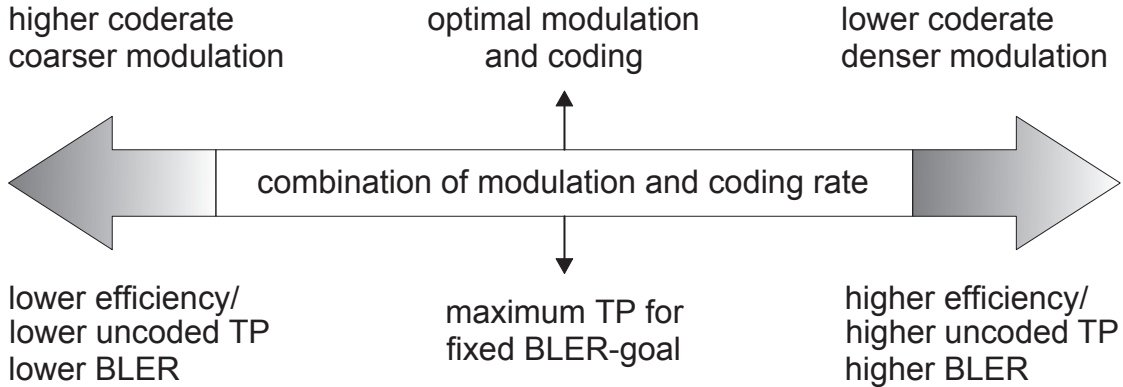


Figure 2.6: Effects of MCS on throughput and BLER.

power) will lead to a higher data rate but also to a higher BLER. To be able to transmit at a close to optimal point, it is viable that the modulation and coding can be adapted, leading to the concept of AMC. For a given setup of transmission parameters, a specific combination of modulation and coding yields a certain performance. These parameters include, e.g., the channel characteristics, the Signal to Interference and Noise Ratio (SINR) and the receiver-performance. By adapting the modulation order and the coderate, the transmission can take place at an optimum point. This is specified as the maximum throughput while guaranteeing a BLER not exceeding a certain threshold [22]. The combinations of

modulation and coding rate, that are defined for LTE are discussed later in the next section.

2.2 LTE MAC-Layer

After the resource-structure has been defined, it is now discussed how it is decided which user transmits his data on what resource and in what fashion, based on the user-specific information that is fed back to the transmitter. The LTE-standard contains several predefined strategies, that are stated at the end of this section.

2.2.1 Feedback

To signal the transmitter the optimal transmit-parameters, there are up to three different values specifying them. They are calculated on the receiver side and fed back to the eNodeB for every active UE individually. All feedback values are only a recommendation to the eNodeB's scheduler. The scheduler can override the values from the UEs but has to signal then, what transmission parameters are used. What feedback strategy is applied depends on the transmission mode. Two strategies are explained in more detail in Section 3.2.1.

Channel Quality Indicator

In LTE, the Channel Quality Indicator (CQI) defines a pair of modulation scheme and code rate. The values range from 0-15 and the corresponding transmission parameters can be found in Table 2.3. Possible modulation schemes (applied on every subcarrier) are 4-QAM, 16-QAM and 64-QAM. The column *efficiency* is calculated as the product of number of coded bits per symbol and the coding rate and describes how many data bits are transmitted in one OFDM-symbol. Therefore, the number of data bits that are transmitted in one RB is calculated as $N_{bits} = cN_S N_{c,RB}$, with c representing the efficiency. How the optimal CQI-value for every RB is chosen, again depends on the transmission mode.

Rank Indicator and Precoding Matrix Indicator

Transmission-modes that support SM require more than the already described CQI-feedback. As discussed above, MIMO allows for the parallel transmission of several transmit-streams, but with a trade-off between diversity gain and multiplexing gain. The number of transmit-layers is also termed *rank* and is represented in the feedback as Rank Indicator (RI). The mapping from transmission layers to

CQI-index	modulation	code rate	efficiency
0	out of range		
1	4-QAM	0.08	0.15
2	4-QAM	0.12	0.23
3	4-QAM	0.19	0.38
4	4-QAM	0.30	0.60
5	4-QAM	0.44	0.88
6	4-QAM	0.59	1.18
7	16-QAM	0.37	1.48
8	16-QAM	0.48	1.91
9	16-QAM	0.60	2.41
10	64-QAM	0.46	2.73
11	64-QAM	0.55	3.32
12	64-QAM	0.65	3.90
13	64-QAM	0.75	4.52
14	64-QAM	0.85	5.12
15	64-QAM	0.93	5.55

Table 2.3: Associated modulation and coding rate for the LTE CQIs [3].

antennas is done with a PM, the optimal one is signalled in the feedback with the Precoding Matrix Indicator (PMI).

2.2.2 Scheduling

The task of the scheduler in a mobile communication system is to handle the access on the media by all active UEs, i.e., fill the resource grid defined in Section 2.1, and is therefore located on the MAC-layer. In LTE, the scheduler uses rate control (in contrast to power control in, e.g., Wideband Code Division Multiple Access (W-CDMA)), what means that the data-rate for a user is adapted to the current channel conditions. This concept has already been introduced in Section 2.1.4, but the difference now is, that the scheduler can choose from a pool of users. Supplied with the user-feedback, the scheduler can use that knowledge to exploit the variations in the channel by adequate choices of resource assignment to the users and the applied MCS. This gain achieved from choosing users with preferable channel conditions is called multi-user diversity. Naturally, the gain is larger for a higher number of users and for channels with large variations. However, in environments with very fast channel-variations (relative to the feedback period and scheduling granularity over time), the feedback information might already be outdated and no longer valid. In such cases, the utilization of HARQ is a viable option, because it implicitly adapts the data rate to one that is supported by the

channel. The position of the scheduler in the protocol stack with its inputs and outputs is shown in Figure 2.7.

Always choosing the users with the best channel conditions for transmission leads

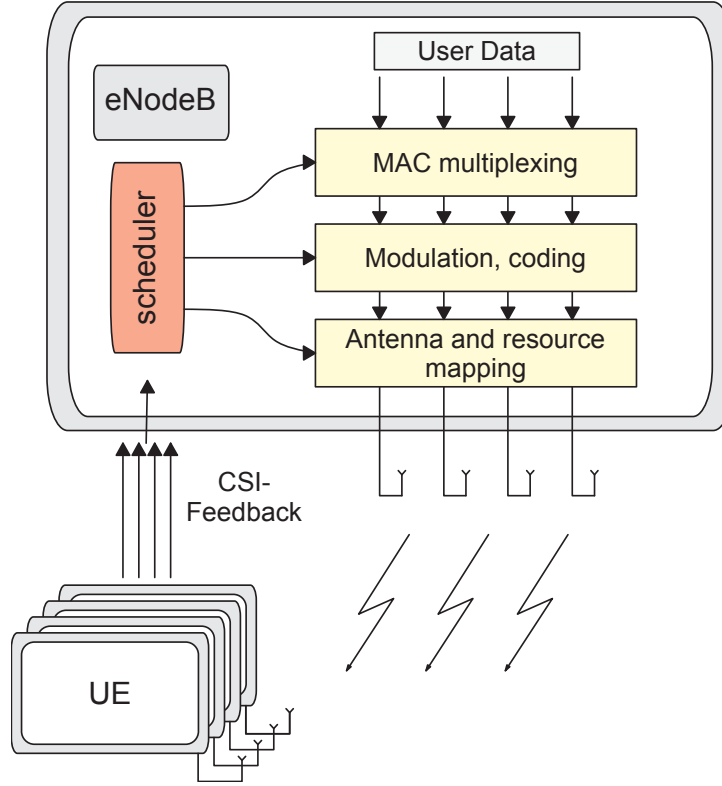


Figure 2.7: Position and role of the scheduler in the protocol stack.

to a maximization of the sum-throughput in the cell. If the average channel quality for all users is about the same, the fairness in the cell will still be high. If however the average conditions for the users vary, it can happen that some users are assigned all resources, while there are none left for users with bad average channel conditions. This leads to a highly unfair situation with many unsatisfied users at the cell-edge. The other extreme represents a Round Robin (RR)-scheduler, that distributes the available resources equally between the users, regardless of their channel state (but applying the appropriate MCS). This leads to a reduced overall efficiency because not the maximum possible CQI for each RB is used. Therefore, a scheduler has to be able to exploit the variations in the channel quality as well as keeping track of the average throughput and guaranteeing a certain minimal performance, in order to satisfy certain Quality of Service (QoS)-constraints. An example for such a scheduler is Proportional Fair (PF)-scheduling [24]. It is left to say that the scheduling strategy is not defined in the standard, only the reference signals and the feedback information. However, the chosen strategy extremely influences the performance of the network.

Mode	Transmission scheme	λ	Release	RS
1	Single-antenna transmission	1	8	CS-RS
2	Transmit diversity	1	8	CS-RS
3	OLSM	2-4	8	CS-RS
4	CLSM	2-4	8	CS-RS
5	CB-based MU-MIMO	2-4	8	CS-RS
6	CLSM single layer	1	8	CS-RS
7	Non-CB-based single layer transmission	1	8	CS-RS & DM-RS
8	Non-CB-based double layer transmission	1-2	9	CS-RS & DM-RS
9	Non-CB-based eight layer transmission	1-8	10	CSI-RS & DM-RS

Table 2.4: Overview of the LTE and LTE-A transmission modes

2.2.3 LTE Transmission-Modes

Multi-antenna transmission in LTE can be performed in different ways. The different options are termed *transmission modes*, an overview can be found in Table 2.4. Not all of the transmission modes shown in the table will be explained here, but only the ones that are of significance for this work.

Reference Signals

In the downlink of LTE, several types of RSs are specified. They consist of a predefined pattern and they are placed on specific positions in the resource grid. RSs are used by the receiving terminals for different purposes. The basic properties are explained in the following.

Cell-Specific Reference Signals: Cell Specific Reference Signals (CS-RSs) were already defined in LTE release 8. They are used by the receiving terminals for both channel estimation and to calculate various Channel State Information (CSI)-values. Their structure allows to distinguish between a maximum number of four antenna-ports.

CSI Reference Signals: CSI Reference Signals (CSI-RSs) were introduced in LTE release 10 and are used in combination with DeModulation Reference Signals (DM-RSs) to calculate CSI-values. In contrast to CS-RSs, there can be up to eight

different CSI-RSs in a cell, therefore allowing for the transmission of up to eight layers in parallel. The period of CSI-RSs can be adjusted between 5 ms and 80 ms. Thus, the amount of overhead can be adapted to the variations of the channel.

DeModulation Reference Signals: DM-RSs are also referred to as User specific RSs, because they are intended for only one specific receive terminal. They are only transmitted in the RBs intended for the specific user. In the case of non-Code Book (CB)-based precoding, DM-RSs are necessary for channel estimation (including the applied precoder) and demodulation. Since the DM-RS are inserted *before* the precoder (in contrast to the other RS), the effective channel $\mathbf{H}_{eff} = \mathbf{H}\mathbf{W}$ can be estimated with these reference symbols with the PM \mathbf{W} being an arbitrary matrix, not necessarily from a CB. The signalling of the precoder-choice in the downlink becomes unnecessary, because the receiver can perform coherent demodulation without knowing the precoder. A user may still feed back a PMI, but since the scheduler takes the final decision about the actual PM, this is only a suggestion.

MIMO-Modes

In Section 2.1.2, it was only explained that transmission of several layers in parallel is possible, but did not clarify, if all layers are intended for the same user or if several users are transmitting on the same RB (same resource in time *and* frequency) in parallel.

Single User MIMO: The term Single User MIMO (SU-MIMO) implies the restriction of the number of scheduled users per RB to one. From a scheduling point of view, the decision is then made solely in the time-frequency domain, it is not possible to transmit data from two or more users in parallel on the same RB. For the choice of the PM, three options are available:

- Open Loop Spatial Multiplexing (OLSM) (mode 3) is used in situations with fast changing channel-conditions. The PMI-feedback outdates too fast to be useful and therefore, the PM-choice is predetermined and it should average the differences in the channel conditions for the different layers.
- Closed Loop Spatial Multiplexing (CLSM) (mode 4,6,9) uses predefined CBs - different codebooks are defined per rank and N_{TX} . For mode 9, also a codebook for up to 8 layers is defined.

- Non-CB-based precoding (mode 7-9) relies on DM-RSs, which are necessary for the user to estimate the effective channel including the precoder (see previous section). Only mode 9 supports up to 8 layers.

Multi User MIMO: When the transmit antennas are used to transmit simultaneously to multiple users on the same RB, one speaks of Multi User MIMO. If every user involved in the MU-MIMO-transmission knows about all transmitted layers and can choose the one intended for him, while discarding the others, it would be the same as spatial multiplexing with the layers intended for different users. This is a very restrictive demand, because every user needs to have at least as many receive antennas as streams. The resource assignment becomes very inflexible, too. However, there are other techniques that do not require knowledge of the entire channel-matrix at the receiver-side. For those, the choice of the precoder plays an integral role and can again be based on a CB or can be an arbitrary PM.

- CB-based MU-MIMO (mode 5,9) tries to minimize the interference between the co-scheduled users by choosing the precoders from the CB with the smallest interference from other users. While already possible for LTE-release 8 with mode 5, the coarse granularity of the CB is the limiting factor in the performance [11]. In LTE-A, two PMI-values are fed back, thus enlarging the number of choices for the PM, making CB-based MU-MIMO a feasible option [17]. A high user diversity is a requirement for a good performance, making it more likely to find matching sets of users.
- Non-CB-based MU-MIMO (mode 7,8,9) relies on the DM-RSs. Since an arbitrary PM can be chosen, this mode does not require a high user-diversity to cancel the interference. It does however require knowledge of the individual channels, experienced by the individual users. Feedback with that information was not defined in release 10. However, with that information available, elaborated MU-MIMO-schemes such as block diagonalization [23] and Zero Forcing (ZF) MU-MIMO [20] become possible. Their goal again is to cancel the interference already at the transmitter. For ZF MU-MIMO, this is done in the eNodeB by choosing the PMs as the pseudo-inverse for the complete channel (including all scheduled UEs). Thus, for perfect channel knowledge, all interference terms are canceled in each UE.

Chapter 3

Measurement Setup and Methodology

Now that the theoretical background has been laid out, the methods and tools for the evaluation and measurement of feedback-based LTE(-A) transmission modes are outlined. After introducing the measurement hardware and the simulation environment, the benefits of the newly enabled realtime feedback by the work described in [19] are shown. With that, the evaluation of more transmission modes becomes possible, which for some has been only possible with very high computational effort and under some constraints or for others has not been possible at all.

3.1 Vienna MIMO Testbed

The Vienna MIMO Testbed is a flexible measurement setup built for performing real-world measurements for arbitrary signals and various wireless transmission standards. It is able to transmit with a maximum bandwidth of 20 MHz over the wireless link. Because the whole testbed is abstracted from the higher layers, it is easy to adapt it to measuring new modes and transmit strategies by changing the input from the higher layers. Its main parts are three transmitter units (called TX1, TX2 and TX3) and one receiver (RX4) and the software that controls the transmission and reception. A short overview of the main parts is given in the following section. Figure 3.1 shows the position of the antennas of TX1, relative to the receiver. Its hardware is located indoors. This transmitter was used for the measurements in Chapter 4.

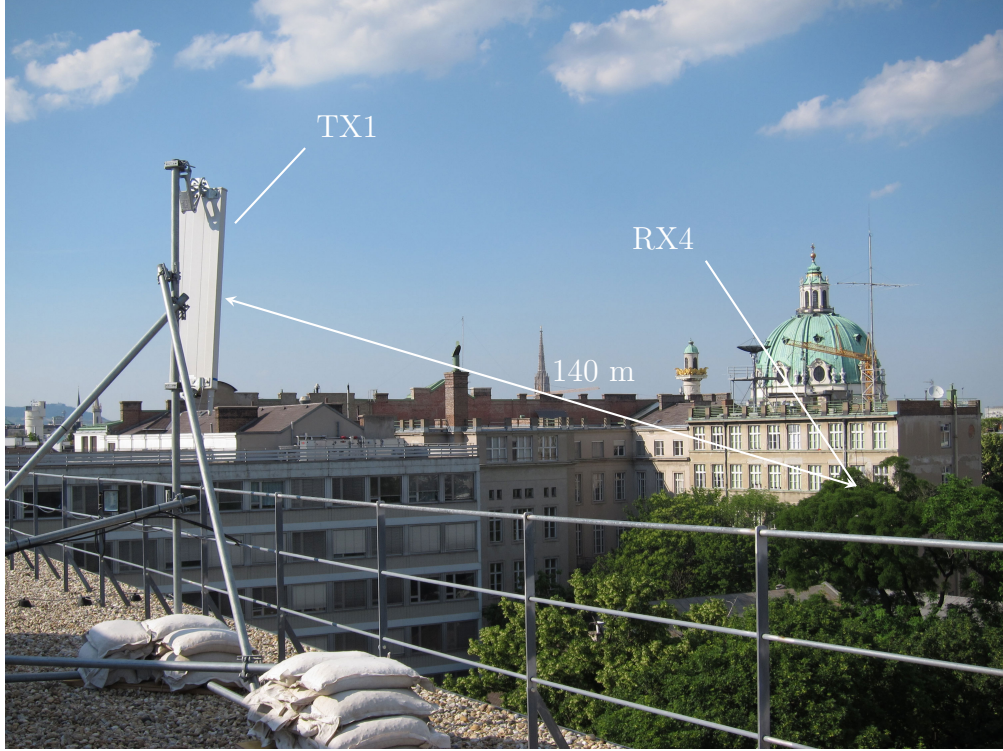


Figure 3.1: Position of the antennas of TX1 relative to RX4, Figure taken from [19].

3.1.1 Hardware

Transmitter: All transmitters are placed at different locations at the Vienna University of Technology. Each of them consists of a consumer PC that houses Digital to Analogue Converter (DAC)-cards, that convert the digital input from the MATLAB-layer into an analogue output signal. This output-signal already is digitally upconverted to an intermediate frequency of 70 MHz and is the input in the RF-stage of the transmitter. This stage consists of the RF-frontend, featuring 4 RF chains with one power amplifier each. The output of this stage finally is fed to the 4 transmit antennas and is radiated at a carrier frequency of 2.5 GHz. To guarantee synchronized clocks, each transmitter has its own GPS receiver as well as a rubidium frequency standard.

Receiver: The receiver-hardware resembles that of the transmitter with slight variations. The signal is received, downsampled and converted by Analogue to Digital Converter (ADC)-cards built into a consumer PC and then stored for later evaluation. Important about the receive antennas is, that they are built into a Notebook housing, which is mounted on an XY Φ -table. Thus, for each measurement a different channel can be realized, varying the small scale fading for every transmission. This is done by moving and rotating the Notebook housing

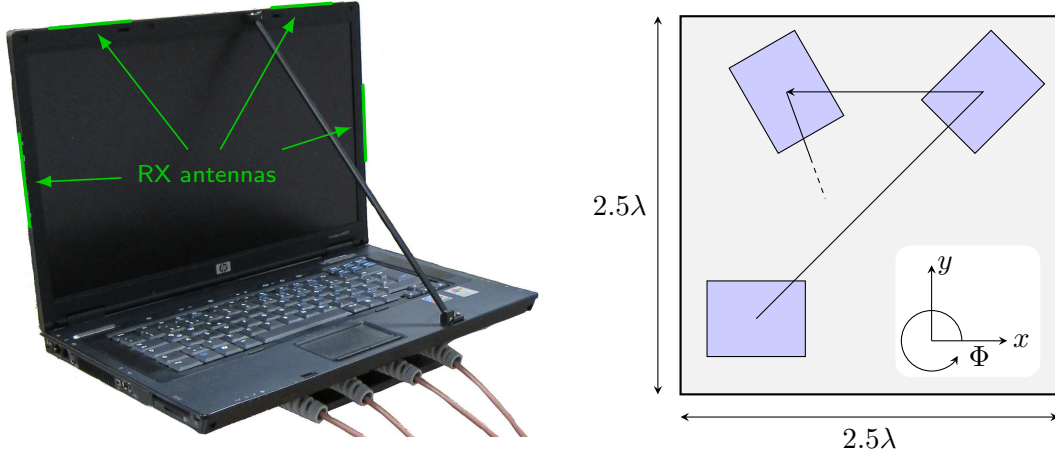


Figure 3.2: The four receive antennas in the Notebook housing, and a schematic of the $XY\Phi$ -table, Figure taken from [19].

on the table, as shown in Figure 3.2.

Further information on the transmitter- and receiver-hardware can be found in [6],[14],[13].

3.1.2 Software

The transmitter- and receiver-hardware is controlled by two server programs, the `TX Daemon` and `RX Daemon` developed in [14] and [13]. These programs themselves are controlled by UDP-packets, e.g., generated by MATLAB. Their main task is to control loading of the data to the DAC-cards in the transmitter and the storage of the data from the ADC-cards in the receiver.

3.2 Simulation Environment

For the measurements, a special MATLAB-program was implemented, handling everything logically above the `TX Daemon` and `RX Daemon` software. A short overview is given in this section.

3.2.1 LTE-Simulator

The Vienna LTE Link Level Simulator [18] is a simulation environment for the simulative investigation of a broad variety of research approaches. The structure of the MATLAB-program, that was used for the measurements and simulations, resembles that of the LTE Link Level Simulator and some of its functions were

directly integrated in the measurement environment, e.g., the feedback-functions or channel-models for measurement-emulation.

CLSM-Feedback: For CLSM transmission modes, a triple of RI, PMI and CQI is calculated at the receiver. To find the optimal combination, the feedback-function in the simulator calculates all SINR values for every OFDM-symbol and for every combination of precoder and rank. For every combination, the according CQI-values are determined. Based on all considered SINRs and on the applied MCS, a corresponding BLER can be predicted. Since a direct mapping from all SINR-values to the resulting BLER is very complex and not flexible, the SINR-values are first mapped to a corresponding effective SINR-value SINR_{eff} . One concept that can be employed to achieve such a mapping is termed Mutual Information Effective SNR Mapping (MIESM). To arrive at a value for SINR_{eff} , the Bit Interleaved Coded Modulation (BICM) capacity [7] of each subcarrier is calculated first, depending on the SINR and the modulation alphabet. Those capacities are then averaged and mapped back to SINR_{eff} , corresponding to an SNR-value for an equivalent Additive White Gaussian Noise (AWGN)-channel. With the help of MIESM, the following procedure is carried out to determine the optimal value:

- Calculate the post equalization SINR for resources of interest
- Map all SINR-values to one average SINR_{eff} with MIESM
- Find the corresponding CQI for SINR_{eff}
- Choose CQI with maximum efficiency for $\text{BLER} \leq 0.1$

What *resources of interest* exactly means is specified by the CQI-feedback granularity. In the feedback-function implemented in the MATLAB-program, consecutive RBs over time are considered together in the feedback, as well as RBs on the same time-frequency resource but on associated layers (according to Table 2.2). For the mapping $\text{SNR} \rightarrow \text{BLER}$, AWGN BLER curves are obtained beforehand by simulation for every MCS. They are shown in Figure 3.3 With the calculated CQI-values for all PMI and RI combinations, a decision can be made by choosing the triple with the highest estimated throughput for a BLER smaller than 0.1 [22].

ZF MU-MIMO Feedback: The CQI-feedback for ZF MU-MIMO is calculated with the assumption, that each user has only one receive antenna. The CQI calculation is taken from [21], where a lower bound for the SINR is derived. For our purposes, a simplified version is used, neglecting all interpolation errors, because

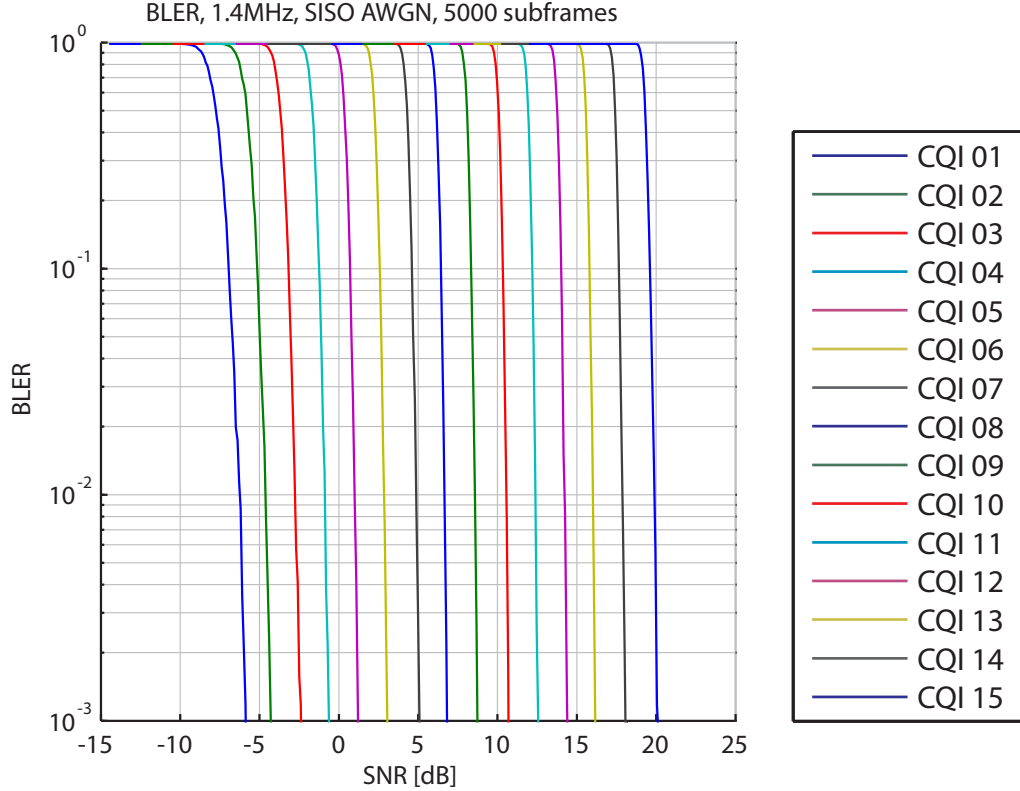


Figure 3.3: BLER per CQI, plotted over SNR for a SISO AWGN channel.

we assume that the channel vector \mathbf{h}_k is unquantized. Transmit power and the norm of the precoding vector are also normalized. This results in the following expression:

$$SINR \geq \frac{1}{N_T} \frac{\|\mathbf{h}_k\|^2}{\sigma_n^2} \quad (3.1)$$

with σ_n^2 representing the noise variance. The CQI-value is corrected for the actual amount of scheduled users after the scheduling (Section 3.4.2).

3.2.2 Simulator - Testbed Interface

The MATLAB-program generates the complete transmit signal, and also has to make sure, that it is compatible with the format required by the DAC-cards. Therefore, the discrete time signal is upconverted and upsampled. Equivalently, in the receiver, the received samples at the output of the ADC-cards have to be downconverted and downsampled. This is done before storing the received samples but also necessary for the feedback-calculation (Section 3.3).

3.2.3 Measurement Emulation

In addition to the measurements, it is also possible to run simulations over a simulated channel, without using the testbed. This is helpful to verify the correct implementation of the measurement software-environment. Therefore, either channel-traces from measurements or the channels can be generated with the link-level simulator, that is able to generate channels for various channel-models, e.g., flat Rayleigh channels or PedA [15].

3.3 Measurement Methodology

Up to now, the measurements with the Vienna MIMO Testbed were executed without the utilization of CSI-feedback (as discussed in Section 2.2.1). To evaluate, which parameters are optimal for transmission, all possible combinations of CQI, RI and depending on the transmission mode also PMI are used for consecutive transmissions. Afterwards, all received data from all transmissions is evaluated and the one parameter-constellation that yields the best results is regarded as the optimal transmission, that could have been achieved with perfect CSI-feedback from the receiver. Figure 3.4 shows a schematic of the described measurement procedure. The three main stages are the following:

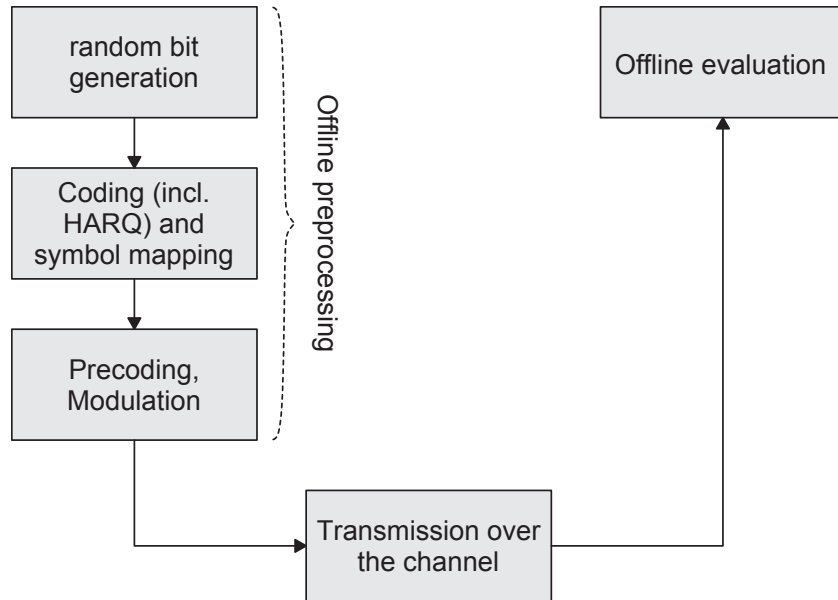


Figure 3.4: Brute force measurement schematic.

1. Generate and preprocess data bits for all necessary transmission-parameter combinations offline and store the readily created time-signals for transmission

2. Perform the transmission for various transmit-power levels and channel realizations (receiver positions) and store the received data
3. Evaluate the received data offline to find the CSI-values with the best results for CQI-, RI- and also PMI-values (depending on the transmission mode)

While relatively simple in execution, there are a number of drawbacks and constraints that stem from the lack of realtime feedback:

- The computational effort for this brute-force approach increases with the number of possible transmission-parameter combinations. Let us consider a 4x4 LTE OLSM transmission (mode 3). For $RI = 1 \dots 4$, the CQI-combinations for codewords on the possible layers equal $15 + 3 \cdot 15^2 = 690$ (see Table 2.2). That means, that for all these combinations, as many subframes have to be transmitted for each power level and receiver position. All received subframes have to be evaluated then, which is also quite time consuming, even if a whole cluster of PCs is combined for this task. Since there is no PMI-feedback for OLSM, there are no additional transmissions necessary for combinations with various PMs. For mode 4 CLSM transmission, there would be an additional factor of 16 for every PM predefined in the codebook and the computational effort would become even less feasible.
- For the evaluation of HARQ-performance, another factor of $N_{RT,max} + 1$ has to be added to the number of necessary transmissions. The retransmissions need to be transmitted, even if the original codeword was received correctly, since the evaluation takes place afterwards and there is no way of knowing online, if that was the case. For smaller setups such as 2x2 mode 2 the additional effort might still be tolerable, but for the aforementioned example, the number of subframes that have to be evaluated gets even more out of hand.
- A user is required to apply the same MCS on all RBs he is assigned to and that belong to one codeword, as defined in the LTE-standard. Therefore, this measurement procedure can be regarded as a single user setup. This one user could be allowed to transmit more than the two codewords defined in the standard. By, e.g., grouping RBs that can support the same CQI together, variations in the frequency domain could be used advantageously. However, the number of necessary transmission would be astronomically high, because now also all permutations over codeword-length and CQI over frequency would have to be transmitted. Thus, the evaluation of channel-dependent

scheduling over time AND frequency is not possible with this measurement procedure.

- The three already stated restrictions arise from an excessive computational effort. The new transmission modes in LTE-A supporting MU-MIMO (see Section 2.2.3) however can not be measured without realtime feedback, because there is no limited number in transmission-parameter combinations anymore.

To overcome these constraints, realtime feedback is made available by the work done in [19], which presents a software extension to the Vienna MIMO Testbed by integrating parts from the Vienna LTE-A Link Level Simulator (see Section 3.2). Based on that, all of the mentioned transmission modes can now also be evaluated with the Vienna MIMO Testbed - how this is done is explained in the following part of the chapter.

3.3.1 Measurement/Simulation Process

To incorporate realtime feedback in the measurements, three new processing steps are introduced:

- Online demodulation of RSs and estimation of the current transmission characteristics
- Calculation of (optimal) CSI-values, based on the information calculated in the first point
- Adaptation of the next transmission at the transmitter according to the CSI from the feedback.

These aspects are visible by comparing Figure 3.4 with Figure 3.5. The new block "Demodulation and estimation" in the new schematic calculates an estimate for the MIMO-channel $\hat{\mathbf{H}}$ (based on the RSs), an estimation for the SNR and an estimation of the Mean Squared Error (MSE) between the true channel \mathbf{H} and the estimated channel $\hat{\mathbf{H}}$. These values are the input-values for the "Feedback calculation" block. The feedback calculation depends on the transmission mode in use. The scheduling block takes the CSI-values from the feedback and passes on the codeword decision to the block "Filling of the resource-grid". How the scheduler interprets the CSI-values again is transmission-mode dependent. Based on the scheduler-output, pregenerated codewords are loaded and the resource-grid is filled accordingly.

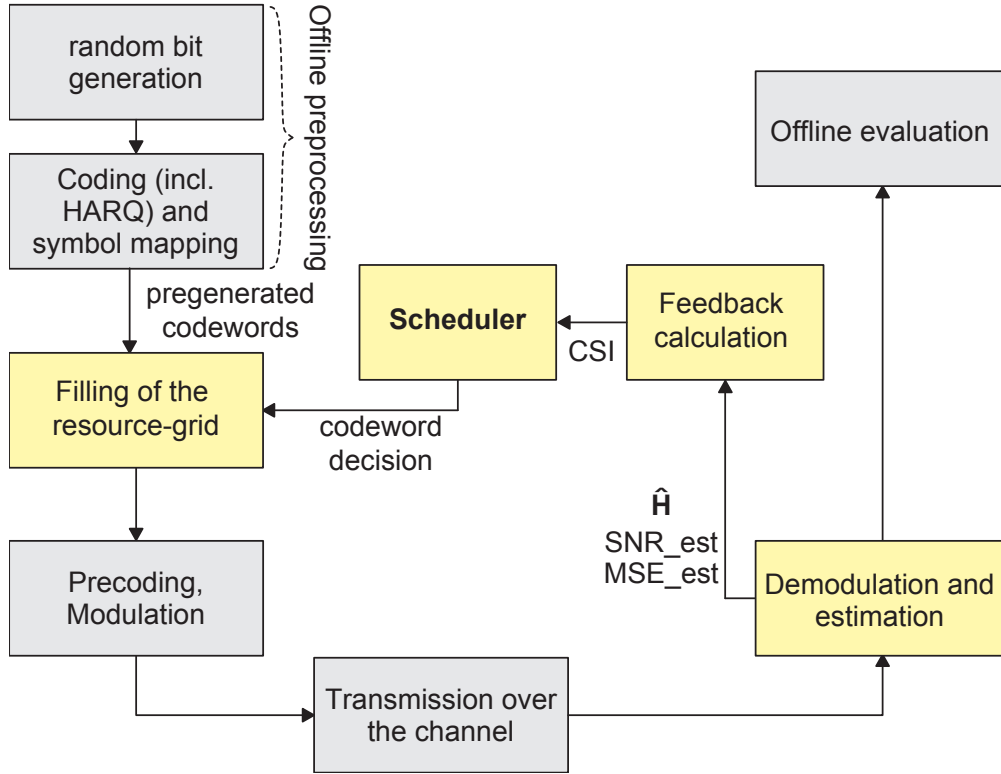


Figure 3.5: Feedback-based measurement schematic.

The time-structure for the transmission of one subframe is shown in Figure 3.6. The first pilot frame consists of a standard-compliant RS, while the rest of the

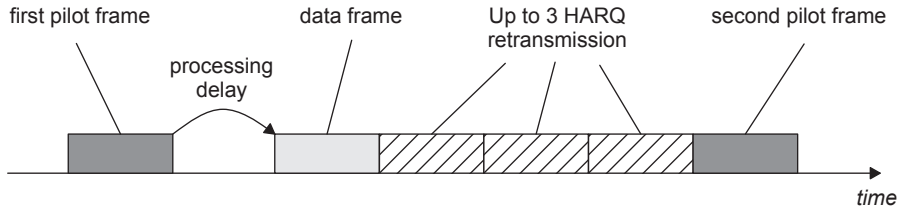


Figure 3.6: Transmission timeline for one measurement-point.

frame is filled up with a much denser pattern of "proprietary" reference symbols, that are used to calculate the channel estimation MSE and to gain almost perfect channel knowledge as a reference to the channel estimate based on the RS. Based on this frame, the feedback input is estimated and then at the transmitter side, the data frame is generated based on the scheduler decision and put together from pregenerated codewords, as explained in the next section. Then, the signal is transmitted over the wireless channel. On the receiver side, the received symbols are not further processed at this stage, but stored for offline evaluation after the transmission.

3.3.2 Data Generation

The gain in flexibility with the new measurement approach comes at the cost of an additional delay, composed of transmission delay on the feedback link, read- and write-times for the data and mostly signal processing. To keep the delay as small as possible, all codewords are precalculated offline. There are three differences in the precalculation of codewords in comparison to the old measurement procedure:

- The randomly generated bits are coded and mapped to the according symbols, but they are not yet precoded and transformed into an OFDM time signal.
- Before, possible codewords did vary in the number of layers ($\lambda = \{1, 2\}$) that they span and in the MCS, but were of fixed length $2 \cdot N_{RB} \cdot \lambda$, leading to $15 \cdot 2$ possibilities. When a frequency dependent scheduler is used, also the length becomes variable.
- Since now also LTE-A measurements can be carried out, and since LTE and LTE-A inhibit a different RS-structure, leading to a different amount of OFDM-symbols available for data-transmission per RB, two different sets of codewords have to be generated for LTE and LTE-A.

For LTE-measurements, the possible length of a codeword L (in RBs) ranges from one to $2 \cdot N_{RB} \cdot \lambda_{max}$, with the maximum of layers being spanned equal to two. However, not all lengths are possible, since the rank is fixed for all RBs of the same user. That means, that a length of $2 \cdot N_{RB} + 1$ is not possible - the next valid length is $2 \cdot N_{RB} + 2$, representing a codeword with $N_{RB} + 1$ RBs, spanning two layers. Therefore, up to a length of $2 \cdot N_{RB}$, pregenerated codewords with even length can be used for two cases: L RBs on one layer or $L/2$ RBs on two layers. Possible values for L therefore are $[1 : 2N_{RB}] \cup [2N_{RB} + 2n], n \in [1; N_{RB}]$. This example is also explained graphically in Figure 3.7. Since the number of CS-RS varies with the number of transmit antennas and thus the number of data-bits per RB, different codewords have to be generated for different numbers of transmit antennas. To give an example, for the maximum bandwidth of 20 MHz (being equal to 200 RBs per subframe), and for four transmit-antennas, $(2N_{RB} + N_{RB}) \cdot 15 = 4500$ different codewords have to be generated, in order to cover all possible options.

The situation for LTE-A is slightly different. First of all, up to eight layers can be transmitted, leading to a maximum codeword-length of $8 \cdot N_{RB}$ (for a codeword spanning the maximum of four layers). Possible values for L for LTE-A are thus $[1 : 2N_{RB}]$, all multiples of two up to $L = 4N_{RB}$, all multiples of three up to

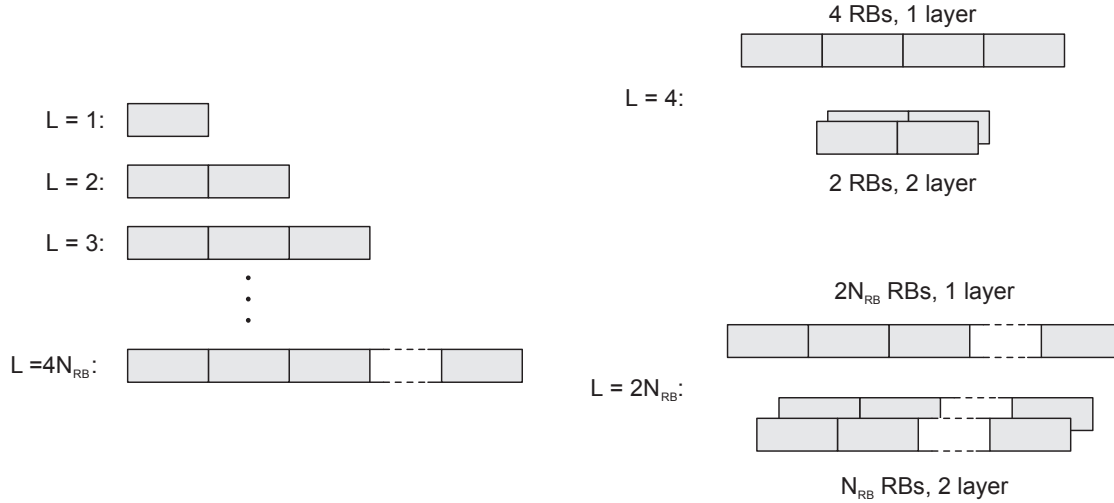


Figure 3.7: Pregenerated codewords; codewords of all possible length are generated, depending on the number of layers, some can be used for different purposes.

$L = 6N_{RB}$ and all multiples of four up to $L = 8N_{RB}$. Again for the example of 20 MHz transmit bandwidth, this results in $484 \cdot 15 = 7260$ possibilities. As for LTE, the RS-structure varies for a different number of transmit antennas and a different set of codewords has to be generated according to that. Moreover does the number of DM-RS depend on the number of layers, which makes it necessary to generate two different codewords for some of the possible values for L .

3.3.3 Offline Evaluation

After all iterations over SNR-values and receiver-positions have been transmitted, there follows the offline evaluation. The evaluation script is structured in three loops as shown in Algorithm 1: Next to the two outer loops over all positions and power levels, there is an inner loop over all codewords received and saved in the according receive file. This inner *for*-loop is executed as long as either all codewords are decoded without error or if all retransmissions have been used. In the algorithm, this is done by the enclosing *while* statement. The variable **ACK** is only true, if all codewords are detected without error, the variable **rv_ii** keeps track on how many of the retransmissions have already been used. In the end, various results are calculated per receive file, e.g., the block errors and the number of successfully decoded bits.

Algorithm 1 Evaluate.m

```
for all TX power levels do
  for all XY $\Phi$ -table positions do
    load Receive File
    while (not (ACK) and (rv_ii < max_retrans)) do
      for all codewords in Receive File do
        if (not NACK_vec(cc) and rv_ii=false) then
          continue
        end if
        Decode all codewords
        Check for Block Error
        Set NACK_vec(cc)
      end for
      Increment rv_ii
      ACK = sum(not (NACK_vec))
    end while
    Calculate and store simulation_results
  end for
end for
```

3.4 Implementation of LTE-Modes

Out of the nine transmission modes introduced in Section 2.2.3, mode 4 and mode 9 have been implemented during this work. The implementation of these modes differs in some aspects, most of which have already been discussed before. An overview from an implementation point of view is given and afterwards, the different scheduler-types are introduced.

3.4.1 Implementation Differences

Mode 4

- **RS Structure:**

Uses CS-RSs; influences pregeneration of codewords, transmit-frame generation, feedback-calculation

- **MIMO:**

CLSM SU-MIMO transmission is used, feedback is calculated with the CLSM feedback-function of the Vienna LTE simulator

- **Scheduler:**

Two schedulers are implemented: *standard compliant*, with a maximum of

two codewords spanning up to two layers each and *frequency selective*, grouping RBs with the same CQI-feedback on the respective layers together in one codeword

Aspects under investigation for mode 4 are HARQ-performance and results for frequency selective scheduling.

Mode 9

- **RS Structure:**

Uses a combination of DM-RSs and CSI-RSs

- **MIMO:**

CLSM SU-MIMO transmission is also implemented, feedback is calculated with the same function as mode 4, exception again for eight layer transmission; additionally, non-codebook-based MU-MIMO based on ZF MU-MIMO is implemented, requiring its own feedback-function and scheduler

- **Scheduler:**

Same two schedulers as for mode 4 can be used, but also the more flexible ZF MU-MIMO-scheduler is available.

For CLSM, a comparison between mode 4 and mode 9 is of interest. The performance of ZF MU-MIMO is also measured, interpreting the 4x4 measurement setup as one eNodeB with four UEs (represented by one receive antenna each).

3.4.2 Scheduler Implementation

The output of the feedback function is used in the scheduler to decide the resource distribution, i.e., how many codewords have to be generated, on what layers they are transmitted and which MCS per codeword is used for the transmission. The layer-to-codeword mapping from Table 2.2 is directly applicable, since only one receiver is present. That means, that also for more than two codewords, they will simply be added up to the sum throughput at the receiver, no association to different UEs takes place. However, considering the 4x4 transmission setup, the number of layers spanned by a single codeword is limited to two. The generic structure of the scheduler output is demonstrated by a representative MATLAB-object:

codeword(x)=

- **UE_scheduled** ($2 \times N_{RB} \times \lambda^x$)
- **CQI** (scalar)
- **layers** (1 or 2 scalars)
- **N_RB** (scalar, 2 to $N_{max} = N_{RB} \times 2 \times 2$)
- **layers_tot** (scalar, 1...4)

UE_scheduled represents the whole resource grid, with logic entries - true if **codeword(x)** is scheduled on that RB and layer, false otherwise. The attribute **CQI** is only a single scalar, since the CQI-values for all RBs belonging to the same codeword are averaged if necessary and replaced by that average value. For that, again MIESM is used (see Section 2.2.1). On which layers the codeword is transmitted is specified in **layers**. Since only a maximum of four layers is possible, two layers are the maximum for one codeword. **N_RB** is simply the length in RBs of the codeword. The total number of transmit-layers is represented by **layers_tot**, ranging from one to four. Additionally a RB-map is generated. For, e.g., three codewords([x,y,z]), this grid would be filled with x where **codeword(x)** was scheduled, RBs assigned to **codeword(y)** with y etc. The number of generated codewords depends on the feedback, but also on the applied scheduler. The details to the three schedulers that have been implemented are introduced in the following.

Scheduler for CLSM

Standard Compliant Scheduler: For the Standard Compliant Scheduler (SCS), the whole measurement setup is interpreted as a single eNodeB - single UE scenario with four transmit and receive antennas each. As a consequence, the codeword-to-layer mapping from Table 2.2 applies, only two codewords are possible. All CQI-values for the RBs of associated layers are averaged by applying MIESM. The feedback values for RI and PMI are adopted unchanged.

Frequency Selective Scheduler: The Frequency Selective Scheduler (FSS) imitates the behavior of a best-cqi scheduler. The CQI-feedback is interpreted as an overlay of several UEs, where always the maximum value among those UEs is chosen (RI- and PMI are supposed to be the same for all UEs). Again the codeword-to-layer mapping is carried out the same way. The difference to the SCS

is now, that all RBs on associated layers with the same CQI-feedback are grouped together and transmitted in one codeword. Thus, adapting the MCS via MIESM becomes unnecessary. If for some RBs the CQI-feedback should be 0, all of those RBs will be transmitted in one codeword with CQI 1. They should not be put together with the RBs with CQI-feedback equal to 1, because a block error is quite likely and thus, the whole long codeword might be lost. This scheduler does not reflect a scenario that can be found in "reality", since all virtual UEs are very close together and experience the same SNR. Still, the effect of a finer granularity in the frequency domain can be investigated.

An example on the working principle of the two CLSM-schedulers is demonstrated in Figure 3.8. Both schedulers get the same input from the feedback-

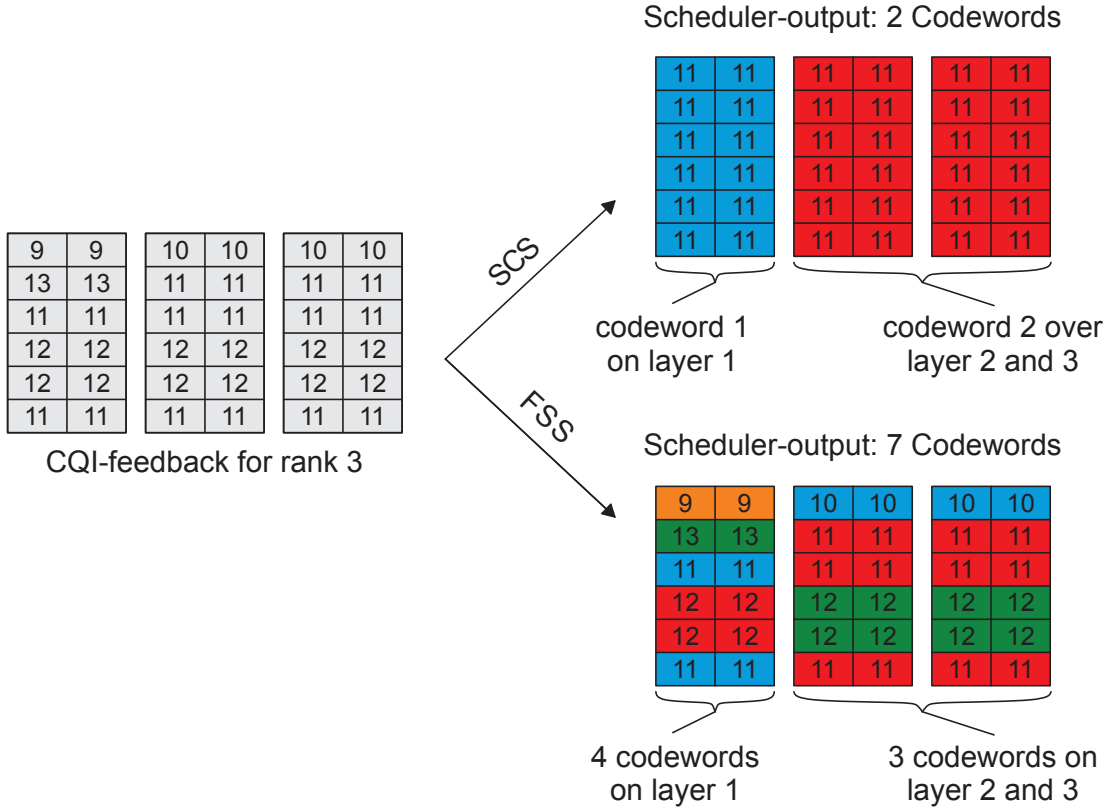


Figure 3.8: Example for the SCS and FSS, based on the same CQI-feedback.

function. The SCS averages the CQI-values of all RBs belonging to the same codeword, i.e., for rank 3 codeword 1 occupies the first layer, codeword 2 layer 2 and 3. The FSS does not change the CQI-values, but groups those RBs with the same CQI on associated layers, which leads to four codewords on the first layer (representing 4 different CQI-values) and three codewords on layer 2 and 3 (three different CQI-values). The attributes of the scheduler-object are then filled

accordingly.

ZF Scheduler

The two schedulers described previously are applicable for mode 4 and 9, CLSM, which implies SU-MIMO. As already described in the previous section, the performance of non-CB-based transmission for mode 9 can be investigated by interpreting every receive antenna as an individual user. A possible scheduling strategy for ZF MU-MIMO is described in [10]. However, the SW-environment was designed for a static rank over the whole RB-grid, which makes it less flexible than required by this ZF MU-MIMO scheduling strategy. As a simplified solution, compatible with the Testbed SW-environment, several simulations with the transmission rank set to a static value $\lambda = 1 \dots 4$ are performed. Thus, the Zero Forcing Scheduler (ZFS) gets a parameter for the constant number of layers to choose and is not able to change it. Since the CQI-feedback for ZF MU-MIMO as stated in Equation (3.1) is always calculated for all four layers individually, the codeword-assignment is one codeword per each chosen layer. Again MIESM is used to average the CQI-value for associated RBs, and the λ layers with the highest average-CQI are chosen. Then the CQI-feedback is corrected to the actual amount of layers by multiplying all SINR-values with a factor $\frac{N_T}{\lambda}$ and the new average CQI-value is calculated per layer. This procedure is clarified in Figure 3.9. In the example, λ was set to three,

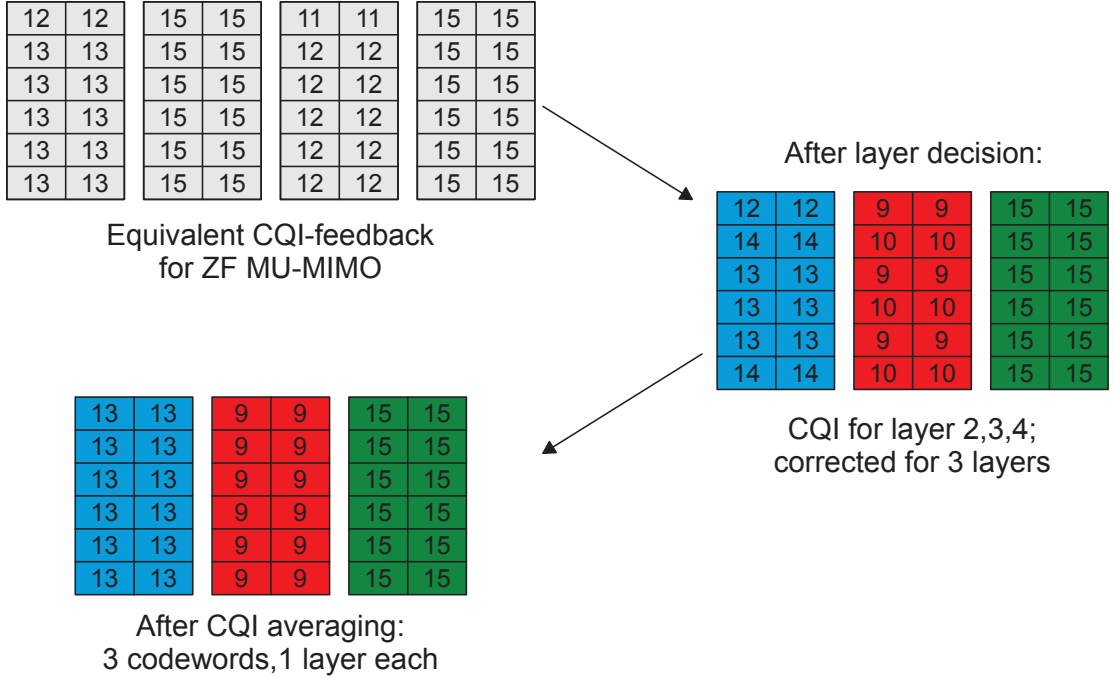


Figure 3.9: Example for the working principle of the ZFS.

the layers with the highest average CQI were layer 2,3 and 4¹. The final output of the scheduler corresponds to three codewords with CQI 13, 9 and 15. On the receiver side, only the signals on antenna 2,3 and 4 are considered and processed individually, as if they were different UEs, but very close together.

¹The equivalent CQI-values are mapped from the unquantized CQI-domain. That means, that the feedback consists of the SINR_{eff} -values per RB. Otherwise, the maximal feedback would be limited to 15 and the CQI-correction leads to wrong results. Since the data-rate over the feedback-link is not limited for the measurement setup, reporting unquantized CQI-values is not a problem. Also the factor $\frac{1}{N_T}$ and N_T cancel, why they are omitted in the actual implementation. The correction is only done by multiplying with $\frac{1}{\lambda}$ and therefore the corrected values are lower than the feedback values.

Chapter 4

Measurement- and Simulation-Results

In this chapter, the results of the measurements are presented and compared to the results of the simulations. For the measurements, TX1 is used as a transmitter. The SNR-range is chosen from -10 dB to roughly 30 dB, where the relation of output-power and SNR is still linear. For the simulations, the ITU PedA channel model is used [15], because it resembles the conditions of the channel for the measurement regarding the long coherence time. The transmit-bandwidth for measurement as well as simulation is set to 1.4 MHz. Table 4.1 sums up all parameters, the results for different configurations are then explained in more detail in the according section.

4.1 Comparison of Different Scheduling Granularities

4.1.1 LTE Transmission-Mode 4, CLSM

For LTE transmission mode 4, CLSM, the SCS and FSS are applicable. Results for coded throughput for both schedulers are shown in Figure 4.1, for simulation as well

System bandwidth	1.4 MHz	Transmission-modes	mode 4 CLSM
Carrier frequency	2.5 GHz		mode 9 CLSM
# of realizations	100	Scheduler	ZF MU-MIMO
MIMO setup	4x4		SCS, FSS, ZFS
Channel	real / PedA		[0,3]

Table 4.1: Measurement- and simulation-parameters.

as measurement. Comparing measurement and simulation results, we see that they

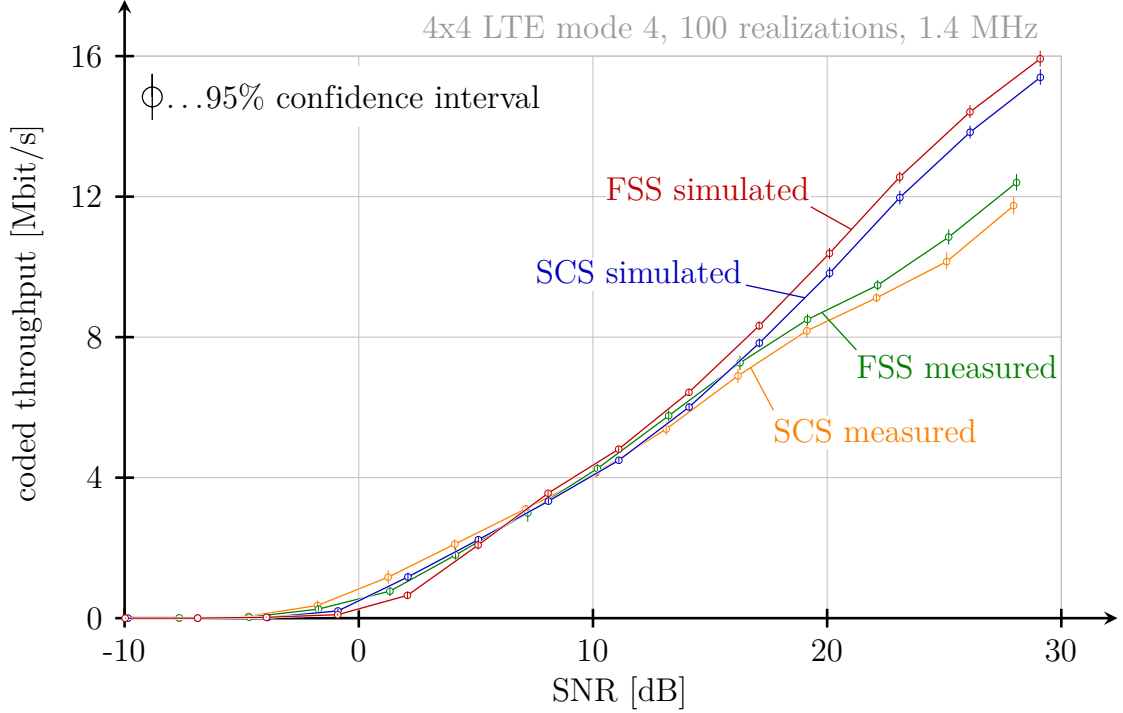


Figure 4.1: Simulation results for coded throughput for LTE transmission mode 4 and 9; results for FSS and SCS are shown.

overlap quite well in an SNR range from roughly -10 dB to 20 dB. Above that, the correlation of the antennas limits the throughput in the measurements. Regarding the two different schedulers, for higher SNR-values, the FSS outperforms the SCS. This gain results because the FSS does not average over whole layers, but uses shorter codewords with appropriate CQI (see Section 3.4.2). On the other hand, the on average shorter codewords lead to a higher BLER for low SNR-values. That is why the SCS surpasses the FSS for low SNR-values.

4.1.2 LTE-A Transmission-Mode 9, CLSM

As stated above, the LTE-A transmission mode 9 is a very flexible mode. However, CLSM is also possible and does not differ much from mode 4. Again, SCS and FSS are used. Results from simulation and measurement for coded throughput are shown in Figure 4.2. For the comparison of simulation and measurement, the same is true as stated for mode 4. The behaviour for the two different schedulers also follows the same argumentation. In the results, the maximum throughput for mode 9 is lower than the one for mode 4. This does not correspond completely to the situation in a real LTE-A-system, because the CSI-RSs in our setup are

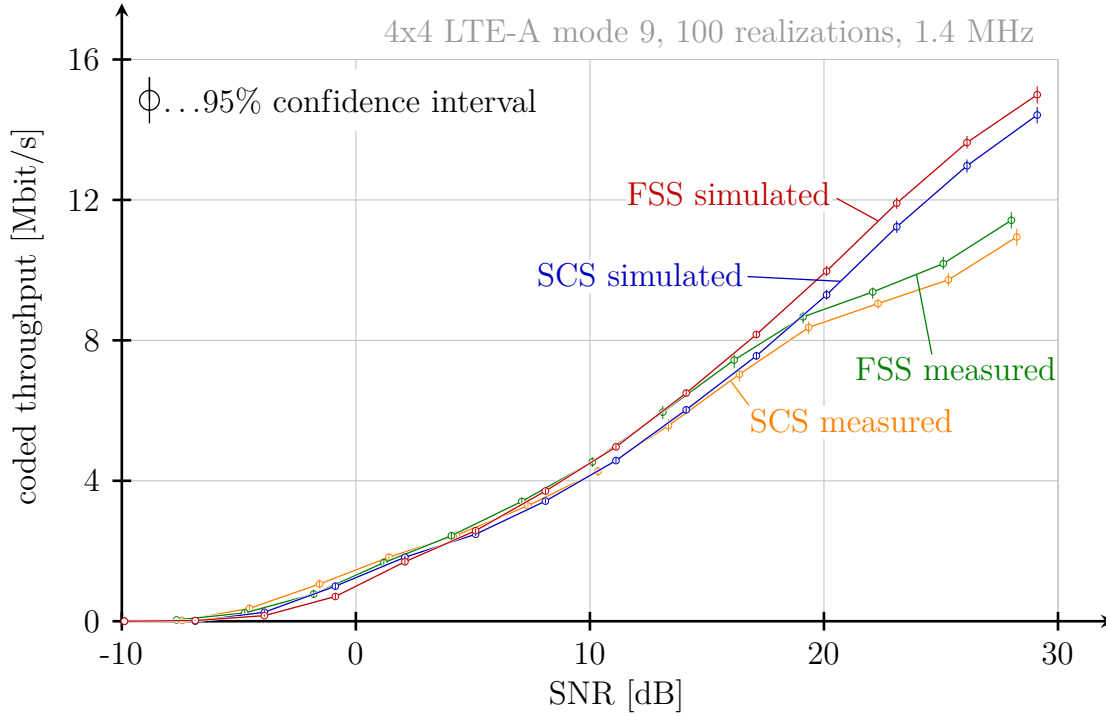


Figure 4.2: Measurement results for coded throughput for LTE transmission mode 4 and 9; results for FSS and SCS are shown.

transmitted in every subframe, not all 5 to 80 ms. Still, the average amount of RS per subframe for a 4x4-setup is larger for LTE-A than for LTE.

4.2 HARQ-Performance

The task of HARQ is not only to improve the average throughput, but also to hide eventual errors from higher layer protocols. In order to show the capabilities of HARQ, simulations and measurements were performed, where the SNR is constantly overestimated by 5 dB. The results for the simulations are shown in Figure 4.3, the measurement-results in Figure 4.4. The results are shown for transmission mode 9, CLSM, in combination with the SCS. Comparing the throughput for regular SNR-estimation with zero retransmissions and a maximum of three retransmissions, only below an SNR of 0 dB a difference is visible. The same is true for the BLER, shown in the right part of the figure. For overestimated SNR without retransmissions, the throughput drops significantly, while on the other hand the BLER does not get below 0.3 even for 30 dB SNR. This situation changes when retransmissions are possible. The BLER-performance is almost as good as the one for normal SNR-estimation, the throughput is only a little bit lower than before. That is, because the effective code rate drops with

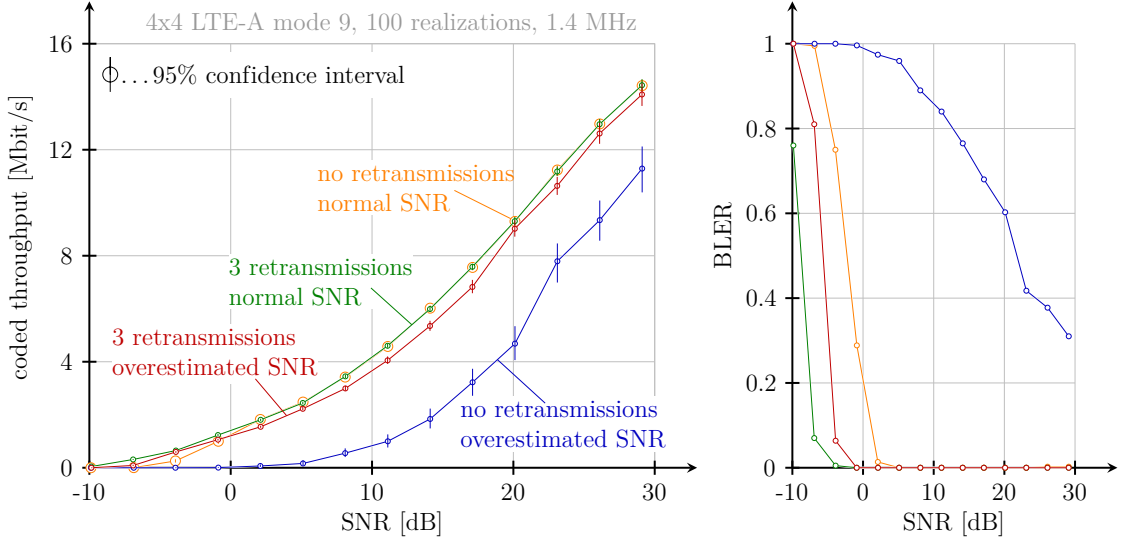


Figure 4.3: Simulation results for coded throughput and BLER with and without HARQ for normal and overestimated SNR.

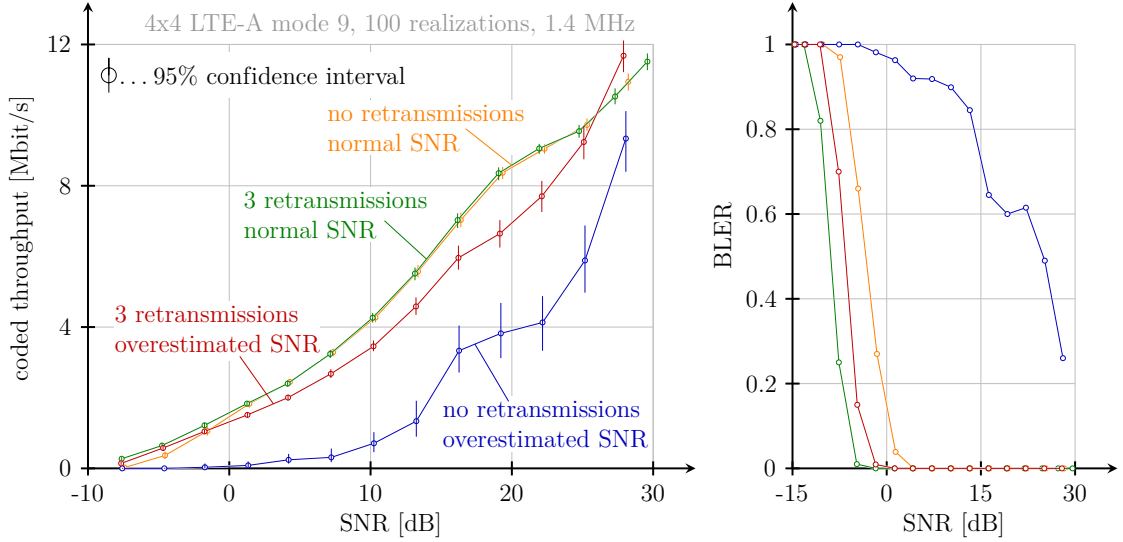


Figure 4.4: Measurement results for coded throughput and BLER with and without HARQ for normal and overestimated SNR.

every retransmission, what increases the amount of actually transmitted bits per data-bit.

For the measurement, the same is true as for the simulation. An interesting point in the measurement-results is, that the throughput for overestimated SNR with retransmission for very high SNR-values is even higher than for the normal SNR-estimation. That results from the feedback being too conservative in that range. The BLER is at zero for both cases, but for the case with overestimated SNR higher CQI- and RI-values are chosen initially. In case of an error, it gets corrected by the retransmissions. The gain from the more optimistic feedback is in

that case higher than the eventual retransmissions reduce the throughput. It is left to say, that these considerations only take the throughput into account, no factors like, e.g., additional delay. The comparison of BLER for the cases with and without HARQ is not really fair, since the BLER for the initial transmission is the same. Thus, this BLER can be regarded as the one that is experienced by a higher layer protocol.

4.3 ZF MU-MIMO

For the ZF MU-MIMO mode, simulations and measurements with fixed numbers of layers are performed. For a 4x4 MIMO-setup, four simulations or measurements are necessary to cover the possible values for $\lambda = 1 \dots 4$. As described in Section 3.4.2, always the λ layers with the highest averaged CQI are chosen for the transmission. The results for coded throughput are shown in Figure 4.5, for the measurements in Figure 4.6.

For the simulation-results as well as for the measurement-result, a fifth curve

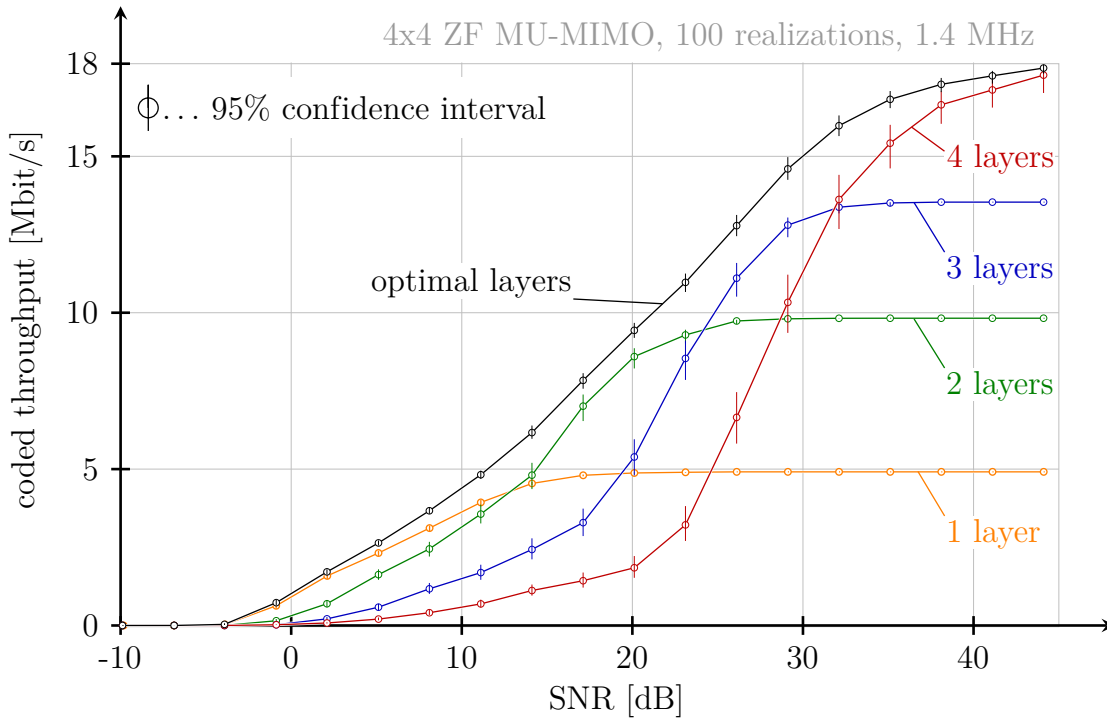


Figure 4.5: Simulation results for coded throughput for ZF MU-MIMO for fixed layers and optimal layer-choice.

is plotted in addition to the four curves corresponding to 1-4 layers. This curve is generated in the evaluation by choosing the number of layers per position and SNR-point, that yields the highest amount of coded bits for this transmission. This

comparison for the simulation is fairer as for the measurements, because there, for each simulation point the same channel and noise realisation is applied, which is not possible for the measurement. Still, also for the measurement, it shows the limits of this mode, if a layer-adaptive scheduler is used, that can decide which number of layers is optimal.

While not improving the throughput compared to the measurement-results for

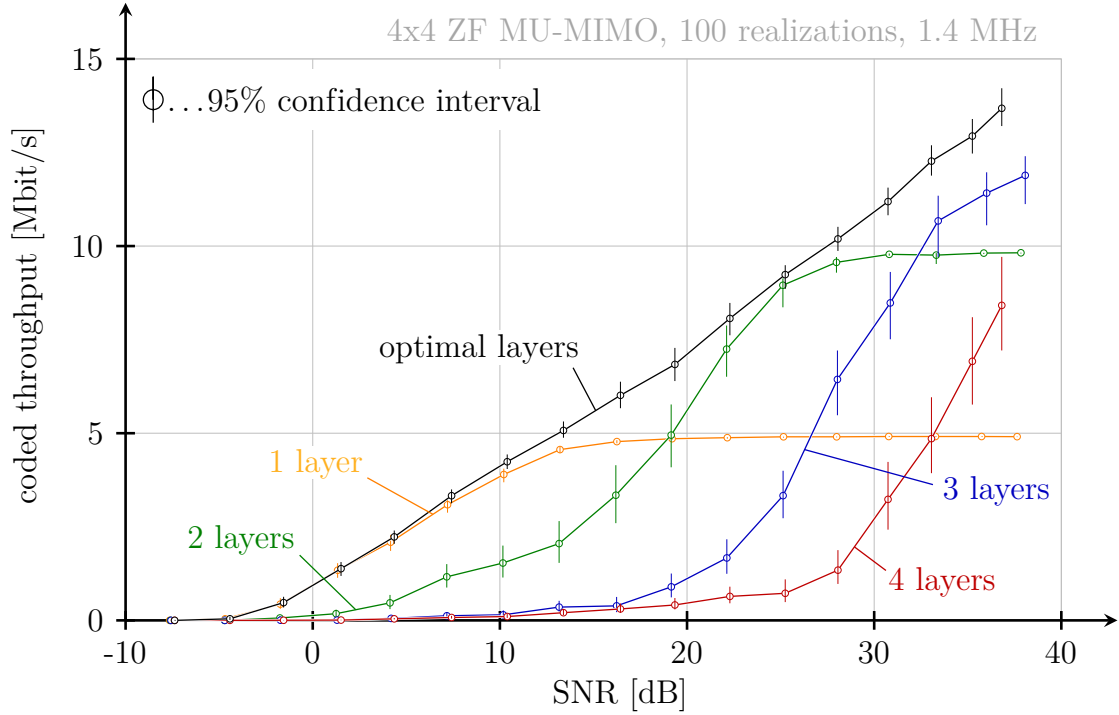


Figure 4.6: Measurement results for coded throughput for ZF MU-MIMO for fixed layers and optimal layer-choice.

mode 9 CLSM, the great benefit of this mode is its flexibility, because only one receive antenna is necessary at each UE for still drawing benefits from the multiple transmit antennas at the eNodeB.

Chapter 5

Conclusion and Outlook

In this work, the LTE and LTE-A transmission modes and features that could not be measured before with the Vienna MIMO Testbed are evaluated by simulation and measurements. This was done by using the feedback-link between the transmitter and receiver of the testbed and incorporating this quasi realtime feedback in the generation of the transmit-signal. One difference to the former measurement procedure is, up to what stage the data can be preprocessed. Before, the time signals were readily available before the transmission started. Now, only codewords of all possible length are generated beforehand. How this is done in an efficient way was also part of this work. Which of those are chosen for transmission is then determined by the newly implemented schedulers, based on the feedback information.

The transmission modes and features, that were evaluated with this new structure are CLSM for LTE and LTE-A, HARQ-performance, frequency selective scheduling and ZF MU-MIMO. For this purpose, three different schedulers have been implemented: the standard compliant scheduler treats the testbed-receiver as one user and allows for only up to two codewords. The frequency selective scheduler groups resources with the same CQI-feedback over the according layers in the same codeword, thus allowing for a higher granularity and exploiting the frequency diversity. The scheduler for ZF MU-MIMO produces one codeword per layer and adapts the CQI, but does not choose the number of layers adaptively. From the transmitter point of view, each receive antenna is seen as an individual user.

For frequency selective scheduling, measurements for larger bandwidth would be of interest, because there the benefit of a finer granularity should be more pronounced. However, the mapping from SNR to CQI is different for, e.g., 10 MHz and 1.4 MHz. Because this mapping did not fit, measurements for 10 MHz resulted

in a BLER > 0.1 up to 30 dB SNR. Thus the mapping has to be adapted for larger bandwidths.

No layer-adaptive scheduler for the ZF MU-MIMO mode has been implemented yet. First attempts have been made to integrate this in the scheduler, based on the approach in [10]. The same scheduling strategy was used to estimate which UEs get assigned on the most subcarriers and how many are scheduled per subcarrier on average. These two values were then the basis for the layer-choice, but the number of layers was overestimated most of the time. A possible way to correct this could be based on using the channel estimation error and the expected interference, or by implementing a more flexible structure, where the number of layers is not fixed for all RBs in one subframe, but can be chosen independently per RB.

Bibliography

- [1] 3GPP. *Technical Specification Group Radio Access Network; (E-UTRA) and (E-UTRAN); Base Station radio transmission and reception ; (Release 10)*. Tech. rep. 07/2013. URL: <http://www.3gpp.org/ftp/Specs/html-info/36104.htm>.
- [2] 3GPP. *Technical Specification Group Radio Access Network; (E-UTRA) and (E-UTRAN); Physical Channels and Modulation; (Release 10)*. Tech. rep. 04/2013. URL: <http://www.3gpp.org/ftp/Specs/html-info/36211.htm>.
- [3] 3GPP. *Technical Specification Group Radio Access Network; (E-UTRA) and (E-UTRAN); Physical layer procedures; (Release 11)*. Tech. rep. 07/2013. URL: <http://www.3gpp.org/ftp/Specs/html-info/36213.htm>.
- [4] S. Alamouti. “A simple transmit diversity technique for wireless communications”. In: *IEEE Journal on Selected Areas in Communications* 16.8 (1998), pp. 1451–1458. DOI: 10.1109/49.730453.
- [5] C. Berrou, A. Glavieux, and P. Thitimajshima. “Near Shannon limit error-correcting coding and decoding: Turbo-codes. 1”. In: *IEEE International Conference on Communications, 1993. ICC '93 Geneva. Technical Program, Conference Record*. Vol. 2. 1993, 1064–1070 vol.2. DOI: 10.1109/ICC.1993.397441.
- [6] Sebastian Caban. “Testbed-based Evaluation of Mobile Communication Systems”. PhD thesis. Institut für Nachrichtentechnik und Hochfrequenztechnik, 2009. URL: http://publik.tuwien.ac.at/files/PubDat_181156.pdf.
- [7] G. Caire, G. Taricco, and E. Biglieri. “Capacity of bit-interleaved channels”. In: *Electronics Letters* 32.12 (1996), pp. 1060–1061. DOI: 10.1049/el:19960754.
- [8] D. Chase. “Code Combining—A Maximum-Likelihood Decoding Approach for Combining an Arbitrary Number of Noisy Packets”. In: *IEEE Transactions on Communications* 33.5 (1985), pp. 385–393. DOI: 10.1109/TCOM.1985.1096314.
- [9] Erik Dahlman, Stefan Parkvall, and Johan Sköld. *4G LTE/LTE-Advanced for Mobile Broadband*. Elsevier Science, 2011.

- [10] G. Dietl, O. Labreche, and W. Utschick. “Channel Vector Quantization for Multiuser MIMO Systems Aiming at Maximum Sum Rate”. In: *Global Telecommunications Conference, 2009. GLOBECOM 2009. IEEE*. 2009, pp. 1–5.
- [11] J. Duplicy, B. Badic, R. Balray, R. Ghaffar, P. Horáth, F. Kaltenberger, R. Knopp, I. Z. Kovács, H. T. Nguyen, D. Tandur, and G. Vivier. “MU-MIMO in LTE Systems”. In: *EURASIP Journal on Wireless Communications and Networking* (2011).
- [12] Leonhard Edlinger. “Vienna Wireless Testbed”. MA thesis. Institute of Telecommunications, Vienna University of Technology, 2012.
- [13] Heinz Haderer. “Wireless Testbed Receiver”. MA thesis. Institute of Telecommunications, Vienna University of Technology, 2012.
- [14] Edin Huremovic. “Wireless Testbed Transmitter”. MA thesis. Institute of Telecommunications, Vienna University of Technology, 2012.
- [15] ITU. *Recommendation ITU-R M.1225: Guidelines for Evaluation of Radio Transmission Technologies for IMT-2000*. Tech. rep. 1997.
- [16] M. Lerch and M. Rupp. “Measurement-Based Evaluation of the LTE MIMO Downlink at Different Antenna Configurations”. In: *Proc. of 17th International ITG Workshop on Smart Antennas (WSA 2013)*. Stuttgart, Germany, 03/2013.
- [17] Chaiman Lim, Taesang Yoo, B. Clerckx, Byungju Lee, and Byonghyo Shim. “Recent trend of multiuser MIMO in LTE-advanced”. In: *Communications Magazine, IEEE* 51.3 (2013), pp. 127–135. DOI: 10.1109/MCOM.2013.6476877.
- [18] *LTE Advanced Link Level Simulator*. URL: <http://www.nt.tuwien.ac.at/research/mobile-communications/lte-simulators/> (visited on 11/08/2013).
- [19] Michael Meidlinger. “Enabling real-time feedback for LTE measurements with the Vienna MIMO Testbed”. MA thesis. Institute of Telecommunications, Vienna University of Technology, 2013.
- [20] J.C. Mundarath and J.H. Kotecha. “Multi-User Multi-Input Multi-Output (MU-MIMO) Downlink Beamforming Systems with Limited Feedback”. In: *Global Telecommunications Conference, 2008. IEEE GLOBECOM 2008. IEEE*. 2008, pp. 1–6. DOI: 10.1109/GLOCOM.2008.ECP.737.
- [21] S. Schwarz and M. Rupp. “Adaptive Channel Direction Quantization - Enabling Multi User MIMO Gains in Practice”. In: *IEEE International Confer-*

ence on Communications (ICC) 2012. Ottawa, Canada, 06/2012, pp. 6947–6952.

- [22] S. Schwarz, M. Wrulich, and M. Rupp. “Mutual information based calculation of the Precoding Matrix Indicator for 3GPP UMTS/LTE”. In: *2010 International ITG Workshop on Smart Antennas (WSA)*. 2010, pp. 52–58. DOI: 10.1109/WSA.2010.5456388.
- [23] S. Shim, Jin Sam Kwak, R.W. Heath, and J.G. Andrews. “Block diagonalization for multi-user MIMO with other-cell interference”. In: *IEEE Transactions on Wireless Communications* 7.7 (2008), pp. 2671–2681.
- [24] Zhishui Sun, Changchuan Yin, and Guangxin Yue. “Reduced-Complexity Proportional Fair Scheduling for OFDMA Systems”. In: *International Conference on Communications, Circuits and Systems Proceedings, 2006*. Vol. 2. 2006, pp. 1221–1225. DOI: 10.1109/ICCCAS.2006.284866.

Appendix A

Acronyms

ACK	positive ACKnowledgment
ADC	Analogue to Digital Converter
AMC	Adaptive Modulation and Coding
ARQ	Automatic Repeat reQuest
AWGN	Additive White Gaussian Noise
BER	Bit Error Ratio
BICM	Bit Interleaved Coded Modulation
BLER	BLock Error Ratio
CB	Code Book
CBI	Code Block
CDMA	Code Division Multiple Access
CLSM	Closed Loop Spatial Multiplexing
CQI	Channel Quality Indicator
CRC	Cyclic Redundancy Check
CS-RS	Cell Specific Reference Signal
CSI	Channel State Information
CSI-RS	CSI Reference Signal
DAC	Digital to Analogue Converter
DM-RS	DeModulation Reference Signal
eNodeB	evolved Node B (equivalent to a base station in LTE-A terminology)

FEC	Forward Error Correction
FSS	Frequency Selective Scheduler
HARQ	Hybrid ARQ
IR	Incremental Redundancy
LLR	Log Likelihood Ratio
LTE	Long Term Evolution
LTE-A	LTE Advanced
MCS	Modulation and Coding Scheme
MI	Mutual Information
MIESM	Mutual Information Effective SNR Mapping
MIMO	Multiple Input Multiple Output
MISO	Multiple Input Single Output
MRC	Maximum Ratio Combining
MSE	Mean Squared Error
MU-MIMO	Multi User MIMO
NAK	Negative AcKnowledgegment
OFDM	Orthogonal Frequency-Division Multiplexing
OFDMA	Orthogonal Frequency Division Multiple Access
OLSM	Open Loop Spatial Multiplexing
PF	Proportional Fair (scheduler)
PM	Precoding Matrix
PMI	Precoding Matrix Indicator
QAM	Quadrature Amplitude Modulation
QoS	Quality of Service
RB	Resource Block
RI	Rank Indicator
RR	Round Robin (scheduler)
RS	Reference Signal

SCS	Standard Compliant Scheduler
SISO	Single Input Single Output
SIMO	Single Input Multiple Output
SINR	Signal to Interference and Noise Ratio
SM	Spatial Multiplexing
SNR	Signal to Noise Ratio
SU-MIMO	Single User MIMO
TB	Transport Block
UE	User Equipment
UMTS	Universal Mobile Telecommunications System
W-CDMA	Wideband Code Division Multiple Access
ZF	Zero Forcing
ZFS	Zero Forcing Scheduler